haematologica

Asciminib stands out as the superior tyrosine kinase inhibitor to combine with anti-CD20 monoclonal antibodies for the treatment of CD20+ Philadelphia-positive B-cell precursor acute lymphoblastic leukemia in preclinical models

by Krzysztof Domka, Agnieszka Dąbkowska, Martyna Janowska, Zuzanna Urbańska, Agata Pastorczak, Magdalena Winiarska, Klaudyna Fidyt, Mieszko Lachota, Elżbieta Patkowska, Łukasz Sędek, Bartosz Perkowski, Jaromir Hunia, Justyna Jakubowska, Beata Krzymieniewska, Ewa Lech-Marańda, Wojciech Młynarski, Tomasz Szczepański, and Małgorzata Firczuk

Asciminib stands out as the superior tyrosine kinase inhibitor to combine with anti-CD20 monoclonal antibodies for the treatment of CD20+ Philadelphia-positive B-cell precursor acute lymphoblastic leukemia in preclinical models

Running title: Asciminib with anti-CD20 mAbs for Ph+ B-ALL

Krzysztof Domka[1,2], Agnieszka Dąbkowska[1,2], Martyna Janowska[1], Zuzanna Urbańska[3,4], Agata Pastorczak[3,4], Magdalena Winiarska[1,2], Klaudyna Fidyt[2], Mieszko Lachota[5,6], Elżbieta Patkowska[7], Łukasz Sędek[8], Bartosz Perkowski[8], Jaromir Hunia[2], Justyna Jakubowska[3], Beata Krzymieniewska[7], Ewa Lech-Marańda[7], Wojciech Młynarski[3], Tomasz Szczepański[8], Małgorzata Firczuk[1,2, #]

[1]Laboratory of Immunology, Mossakowski Medical Research Institute Polish Academy of Sciences, Warsaw, Poland

[2]Department of Immunology, Medical University of Warsaw, Warsaw, Poland

[3]Department of Pediatrics, Oncology and Hematology, Medical University of Lodz, Lodz, Poland

[4]Department of Genetic Predisposition to Cancer, Medical University of Lodz, Lodz, Poland

[5]Laboratory of Cellular and Genetic Therapies, Medical University of Warsaw, Warsaw, Poland

[6]Department of Ophthalmology, Children's Memorial Health Institute, Warsaw, Poland

[7]Department of Hematology, Institute of Hematology and Transfusion Medicine, Warsaw, Poland

[8]Department of Pediatric Hematology and Oncology, Zabrze, Medical University of Silesia, Katowice, Poland

[#]corresponding author: Małgorzata Firczuk, email: mfirczuk@imdik.pan.pl, Laboratory of Immunology, Mossakowski Medical Research Institute Polish Academy of Sciences

Authors contributions

KD: conceptualization, investigation, methodology, data analysis, visualization, writing and editing. AD, MJ, ZU: investigation, methodology, visualization, contribution to manuscript writing. AP: patient sample collection, data analysis and interpretation, conceptualization. MW: conceptualization, writing and editing. KF, ML: conceptualization, investigation, methodology, contribution to manuscript writing. EP: patient sample collection, investigation. LS, BP: patient data acquisition and analysis, contribution to manuscript writing. JH, JJ: investigation. BK: patient data acquisition and analysis. ELM, WM, TS: providing clinical and patient data, manuscript revision. MF: conceptualization, data analysis and interpretation, resources, supervision, funding acquisition, visualization, project administration, writing and editing. All authors have read and accepted the final version of the manuscript.

Data-sharing statement

Original data used in this study is available from the corresponding author upon request.

in vitro phagocytosis model. Special thanks also go to lab technician Karolina Siudakowska for her invaluable support in PBMC isolations and support in experiments. We extend our sincere thanks to all the patients who graciously donated the primary material used in this study.

 Disclosures

EP received consulting fees from KCR and honoraria from Astellas Pharma, Servier, Amgen, and Novartis for lectures and consulting - all unrelated to the submitted work. The other authors have no competing financial interests to declare.

Abstract

Philadelphia chromosome-positive B-cell precursor acute lymphoblastic leukemia (Ph$^+$ BCP-ALL) is a high-risk acute lymphoblastic leukemia subtype characterized by the presence of *BCR::ABL1* fusion gene. Tyrosine kinase inhibitors (TKIs) combined with chemotherapy are established as the first-line treatment. Additionally, rituximab (RTX), an anti-CD20 monoclonal antibody (mAb) is administered in adult BCP-ALL patients with ≥20% of CD20$^+$ blasts. In this study, we observed a marked prevalence of CD20 expression in patients diagnosed with Ph$^+$ BCP-ALL, indicating a potential widespread clinical application of RTX in combination with TKIs. Consequently, we examined the influence of TKIs on the antitumor effectiveness of anti-CD20 mAbs by evaluating CD20 surface levels and conducting *in vitro* functional assays. All tested TKIs were found to uniformly downregulate CD20 on leukemic cells, diminishing the efficacy of RTX-mediated complement-dependent cytotoxicity. Interestingly, these TKIs displayed varied effects on NK cell-mediated antibody-dependent cytotoxicity and macrophage phagocytic function. While asciminib demonstrated no inhibition of effector cell functions, dasatinib notably suppressed the anti-CD20-mAb-mediated NK cell cytotoxicity and macrophage phagocytosis of BCP-ALL cells. Dasatinib and ponatinib also decreased NK cell degranulation *in vitro*. Importantly, oral administration of dasatinib, but not asciminib, compromised NK cell activity within patients' blood, determined by *ex vivo* degranulation assay. Our results indicate that asciminib might be preferred over other TKIs for combination therapy with anti-CD20 mAbs.

Introduction

B cell precursor acute lymphoblastic leukemia (BCP-ALL) is a genetically heterogeneous malignancy characterized by an uncontrolled proliferation of immature B cells. In recent years, there has been notable progress in diagnosing and treating BCP-ALL, thanks to advanced sequencing techniques and the emergence of new immunotherapies. This led to substantial improvements in treatment outcomes for the majority of children with BCP-ALL. However, due to a higher occurrence of adverse genetic subtypes in adult BCP-ALL, over 40% of adults experience relapses, often refractory to current treatments [1,2]. One of the most prevalent aggressive subtypes of BCP-ALL is characterized by the presence of the breakpoint cluster region-Abelson (*BCR::ABL1*) translocation, also known as the Philadelphia chromosome (Ph$^+$ BCP-ALL). This subtype is treated with tyrosine kinase inhibitors (TKIs) specifically targeting the ATP-binding site of ABL1. Originally developed for chronic myelogenous leukemia (CML), TKIs include first-generation drug imatinib, second-generation TKIs such as dasatinib and nilotinib, which more effectively inhibit BCR::ABL1 mutated variants, as well as the third-generation ponatinib which addresses the T315I mutation in the *ABL1* gene [3]. In addition, in 2021, a novel TKI, asciminib, was approved for CML treatment. Asciminib is an allosteric inhibitor that binds to the myristoyl pocket, effectively inhibiting BCR::ABL1 activity, even in the presence of the T315I mutation [4]. While in CML monotherapy with a TKI is typically effective, Ph$^+$ BCP-ALL patients require combination therapy of TKIs with classical chemotherapeutics, and still, a substantial fraction of patients experiences disease recurrence [5]. Therefore, efforts are underway to actively seek further optimizations in treatment protocols to improve patient outcomes.

One of the strategies in this pursuit is the addition of anti-CD20 monoclonal antibodies (mAb) to chemotherapy regimens and TKI treatment. The phase 3 trial conducted in Ph$^-$ BCP-ALL patients expressing CD20 revealed the significant benefit of adding rituximab (RTX), the anti-CD20 mAb, to chemotherapy [6]. These findings influenced contemporary treatment protocols, where RTX is now integrated into all phases of treatment for adult BCP-ALL patients

exhibiting at least 20% CD20^{+} lymphoblasts [7]. Consequently, CD20^{+} Ph^{+} BCP-ALL patients receive a combination therapy comprising chemotherapy, TKIs, and RTX [8]. Anti-CD20 mAbs kill target tumor cells through several mechanisms, including complement-dependent cytotoxicity (CDC), antibody-dependent cellular cytotoxicity (ADCC), antibody-dependent cell-mediated phagocytosis (ADCP), as well as direct induction of cell death [9,10]. Importantly, the presence of CD20 on the surface of tumor cells is a prerequisite for all these mechanisms to function effectively.

CD20 is a B cell-specific antigen whose expression begins at the pre-B cell stage and persists into mature B cells [11–14]. At diagnosis, CD20 expression is observed in up to 50% of BCP-ALL cases, typically at moderate levels [12,15]. Some chemotherapeutic agents used in BCP-ALL treatment regimens have been demonstrated to modify CD20 expression in lymphoid cells [16,17]. Corticosteroids, essential drugs given in the induction phase of the therapy, were shown to upregulate CD20 *in vitro* and are considered a key factor contributing to CD20 upregulation observed in BCP-ALL patients after the induction phase [18]. Conversely, certain TKIs have been found to significantly decrease CD20 protein levels in B cell lymphoma cells [19]. Moreover, dasatinib has been shown to inhibit immune effector cytotoxicity by targeting SRC family kinases (SFK), which play a pivotal role in transmitting activating signals within immune effector cells necessary for ADCC [19–23]. Despite the ongoing clinical use of combination therapy involving RTX, chemotherapy, and TKIs in CD20^{+} Ph^{+} BCP-ALL patients, comprehensive preclinical investigations into the impact of different TKIs on the performance of anti-CD20 mAbs are currently lacking.

In this study, we found that CD20 is more frequently present in Ph[+] BCP-ALL than in other subtypes, therefore, in adult patients TKIs are commonly administered in conjunction with anti-CD20 mAbs. Hence, we investigated the impact of first-, second-, and third-generation TKIs, along with a novel, allosteric TKI asciminib, on the expression levels of CD20 on Ph[+] BCP-ALL

cells and the function of effector immune cells essential for mAbs activity. While all tested TKIs reduced CD20 expression on the surface of BCP-ALL cells and diminished RTX-mediated-CDC, their effects on ADCC and ADCP varied. Our findings revealed that among the four TKIs examined, asciminib presented the most favorable profile. These results remained consistent across all *in vitro* functional assays and were further validated through *ex vivo* assays, which reflect the actual microenvironment found in the peripheral blood of leukemic patients.

Methods

BCP-ALL patients

Adult patients were diagnosed and treated according to Polish Adult Leukemia Group guidelines (PALG) and pediatric patients according to the modified AIEOP-BFM 2017 protocol (NCT03643276) or EsPhALL2017/COG AALL1631 (EudraCT 2017-000705-20), and as described in [24]. The primary sample collection protocol was approved by the Bioethics Committee of Institute of Hematology and Transfusion Medicine in Warsaw (52/2019, 24/2022) and the Bioethics Committee of Medical University of Lodz (RNN/208/20/KE). Informed written consent was obtained from all participants and/or their parents. Mononuclear cells from the bone marrow were isolated and processed within 24 h of the sample collection.

ADCP assay

$CD20^+$ BCP-ALL patient-derived xenograft cells (PDXs), prestained with CFSE (ThermoFisher Scientific) and opsonized with 5 µg/mL RTX or 5 µg/mL cetuximab (anti-EGFR mAb acting as background control) as well as M1 macrophages differentiated from healthy donors' monocytes were separately preincubated for 2 hour at 37°C with Cmax and ¼ of Cmax concentrations of TKIs. BCP-ALL cells were then transferred to the corresponding macrophage wells and co-incubated with macrophages for 1 h. The macrophages were subsequently stained with CD11b-APC-Cy7 antibody and analyzed by flow cytometry. Immunophagocytosis was assessed as the

percentage of CFSE$^+$ CD11b$^+$ cells in each sample. Next, for each RTX-incubated sample, the background (cetuximab-mediated phagocytosis) was subtracted, and the percentage of phagocytosis was normalized to the highest technical replicate per macrophage donor.

Ex vivo degranulation assay

We enrolled Ph$^+$ BCP-ALL and CML patients treated at the Institute of Hematology and Transfusion Medicine in Warsaw as well as Department of Hematology, Transplantation and Internal Medicine, Central Clinical Hospital University Clinical Center, Medical University of Warsaw. Patients' material was obtained following informed written consent and approval of the Bioethics Comitee of Institute of Hematology and Transfusion Medicine in Warsaw (52/2019 and 24/2022). Peripheral blood samples were collected into a VACUETTE® Blood Collection Tubes coated with heparin at two time points: before TKI administration and 1 hour after oral administration of imatinib (400 mg), dasatinib (100 mg or 140 mg) or asciminib (2 x 40 mg). In case of three patients, additional samples were also collected 24 hours after dasatinib administration and 12 hour after the second dose of asciminib administration, before the delivery of a subsequent dose. A total of 150 µL of blood per replicate was pipetted onto a well plate with 400,000 K562 target cells. Next, anti-CD107a APC antibody with GolgiStop™ Protein Transport Inhibitor (BD Biosciences San Jose, CA, USA) were added to each well. The cells were then incubated for 4 hour in 37°C. Next, red blood cells were lysed using BD Lysing Buffer (BD Biosciences). The cells were stained using BD Fixable Viability Stain 510 (BD Biosciences) and antibodies against CD56 and CD3. The percentage of degranulation was calculated in live CD56$^+$CD3$^-$ cells after subtraction of background - samples with blood but without K562 target cells.

Results

Ph$^+$ BCP-ALL cases commonly exhibit CD20 positivity

To compare CD20 expression in different BCP-ALL genetic subtypes, we evaluated the *MS4A1* mRNA levels in primary BCP-ALL cells by RT-qPCR. In the analyzed cohort of 130 pediatric and adult patients, we observed the highest levels of *MS4A1* mRNA in the Ph[+] subtype (**Fig. 1A**). As the clinical decision about the inclusion of RTX into the treatment protocol for adult BCP-ALL patients is based on the percentage of CD20^{+} subpopulation detected by flow cytometry, we analyzed the percentages of CD20^{+} lymphoblasts in a flow cytometry data collected at BCP-ALL diagnosis. In the Ph^{+} group, the median percentage of CD20^{+} cells was significantly higher compared to all other subtypes combined into the Ph^{-} group. Notably, it exceeded the predefined CD20-positivity cutoff value of 20% (**Fig. 1B**). As shown in **Fig. 1C**, the majority of patients diagnosed with Ph^{+} BCP-ALL were classified as CD20^{+}. We also observed a moderate but significant correlation between *MS4A1* mRNA and surface CD20 protein levels (**Suppl. Fig. 1A**). In addition to Ph[+], hyperdiploid, B-other, iAMP21, and Ph-like genetic subtypes were most often represented in the group of pediatric BCP-ALL patients with the highest CD20 levels (**Suppl. Fig. 1B;** the clinical characteristic of pediatric BCP-ALL patients is summarized in **Suppl. Table 5**). Accordingly, CD20 expression in BCP-ALL cell lines corresponded with observations made on primary cells (**Suppl. Fig. 2**). These results suggest that due to the higher frequency of CD20 positivity in Ph[+] BCP-ALL patients, combination therapy with anti-CD20 mAbs along with TKIs and chemotherapeutics is often utilized in adult BCP-ALL treatment and may also be considered for the treatment of pediatric Ph[+] BCP-ALL.

TKIs promote the downregulation of CD20 in Ph[+] BCP-ALL

CD20 levels may affect the efficacy of anti-CD20 mAbs against hematological malignancies [25–27]. Considering the frequent occurrence of CD20^{+} phenotype in Ph^{+} BCP-ALL at diagnosis, we investigated how the drugs commonly used in the treatment of Ph^{+} BCP-ALL affect CD20 levels. First, we compared the levels of CD20 at the time of diagnosis and after 15 days of the induction phase of chemotherapy (MRD15), which is the first time-point of minimal residual disease assessment in the pediatric BCP-ALL patients. The administered induction treatment regimen

9

(characterized in detail in Supplementary Tables 1 and 2) consisted of drugs including corticosteroids, l-asparaginase, vincristine, daunorubicin, methotrexate, and in case of Ph$^+$ BCP-ALL – imatinib. While in unselected cohort of BCP-ALL patients the CD20 levels were significantly higher at MRD15 as compared with the corresponding samples assessed at diagnosis (**Fig. 2A**), it was not the case in the group of Ph$^+$ BCP-ALL patients (**Fig. 2B**). Similar effects were observed in adult patients' cohort (**Suppl. Fig. 3**) who received induction treatment regimens consisting of aforementioned drugs and liposomal cytarabine, as presented in details in Supplementary Tables 3 and 4. Next, we analyzed the levels of CD20 protein in Ph$^+$ BCP-ALL cells incubated *in vitro* with drugs used in the treatment of Ph$^+$ BCP-ALL patients for 48 h. Our findings revealed a consistent decrease in CD20 levels following exposure to all four TKIs in three out of four tested cell lines (**Fig. 2C, upper panel, Suppl. Fig. 4A**). Additionally, when Ph$^+$ BCP-ALL PDXs were incubated with dasatinib, we observed a reduction in CD20 levels in all five PDXs and in three out of five PDXs after treatment with any of the TKIs (**Fig. 2C, lower panel**, **Suppl. Fig. 4B**). To further explore the mechanism of CD20 downregulation by TKIs, we assessed their impact on *MS4A1* mRNA levels in BCP-ALL cells. All tested TKIs significantly reduced *MS4A1* mRNA levels in BV173 cells, indicating transcriptional downregulation (**Fig. 2D**). Likewise, we found a decrease in CD20 protein amounts in lysates of BV173 cells incubated with all tested TKIs (**Suppl. Fig. 5**). In contrast, several chemotherapeutic drugs, such as L-asparaginase (LASP), daunorubicin (DNR), vincristine (VCR), cytarabine (ARAC), exhibited a contrasting effect, leading to an upregulation of CD20 levels (**Fig. 2E**). Overall, these findings suggest that drugs used in the treatment of Ph$^+$ BCP-ALL differentially affect CD20 levels, highlighting potential implications for Ph$^+$ BCP-ALL treatment with anti-CD20 mAbs.

Ph$^+$ BCP-ALL cells preincubated with TKIs exhibit reduced sensitivity to CDC and ADCC

Given the prominent CD20 downregulation by TKIs, we next examined how these drugs affect the antitumor efficacy of anti-CD20 mAb RTX. To this end, we preincubated Ph$^+$ BCP-ALL cells with TKIs for 48 hours and evaluated their sensitivity to RTX-mediated effector mechanisms

(**Fig. 3A**). Firstly, we assessed RTX-mediated CDC, which relies heavily on CD20 levels[28,29]. Accordingly, all tested TKIs significantly decreased the serum-induced lysis of RTX-opsonized BV173 cells (**Fig. 3B**). A similar reduction in RTX-mediated CDC was observed on PDX cells (**Suppl. Fig. 6A**), but it reached statistical significance only for imatinib and dasatinib.

In subsequent steps, we tested the effects of TKIs on RTX-mediated ADCC. In these experiments, BV173 cells were preincubated with maximal serum concentration (Cmax) and ¼ Cmax concentrations of TKIs, and then co-incubated with a CD16-expressing NK92 cell line in the presence of TKIs for 4 hours to evaluate ADCC. At Cmax concentrations, dasatinib and ponatinib significantly reduced the RTX-mediated cytotoxicity of NK92 cells (**Fig. 3C**), whereas at ¼ Cmax concentrations, only dasatinib did (**Suppl. Fig. 6B**). No reduction of cytotoxicity was observed in imatinib- and asciminib-treated samples (**Fig.3C, Suppl. Fig. 6B**). In summary, these results demonstrate that TKIs induce substantial CD20 downregulation in Ph[+] BCP-ALL cells and reduce their susceptibility to RTX-mediated CDC. However, despite similar reductions in CD20 levels mediated by all TKIs, only dasatinib and ponatinib diminished RTX-mediated ADCC.

Cytotoxic activity of effector cells is preserved in the presence of asciminib and imatinib

Based on the above results we hypothesized that the inhibitory effect of selected TKIs on ADCC may be predominated by their impact on the effector cells rather than by their effects on CD20 reduction on target tumor cells. To address this hypothesis, we tested the influence of TKIs on ADCC in another variant, when the leukemic cells were co-incubated for 4 hours with cytotoxic effector cells, anti-CD20 mAbs, and TKIs, without any preincubation of target cells with TKIs (**Fig.3D**). Importantly, after 4 h-incubation, the influence of TKIs on CD20 levels in target cells is minimal (**Suppl. Fig. 6C**). Interestingly, results from co-incubation (**Fig. 3E, left panel, Suppl. Fig. 6D, E**) and pre-incubation (**Fig. 3C**) variants were very consistent, thus suggesting that the inhibitory effects of dasatinib and ponatinib on ADCC are mediated mainly by blocking effectors, rather than by downregulating CD20 on leukemic cells. To further delve into these findings, we

11

employed another Ph$^+$ BCP-ALL cell line, SD1, in which TKIs do not downregulate CD20 (**Fig. 2C**), and used peripheral blood mononuclear cells (PBMCs) isolated from healthy donors as the effectors. In these settings, only dasatinib significantly reduced the cytotoxicity of immune effectors, at both Cmax and ¼ Cmax TKIs concentrations (**Suppl. Fig. 6E**). The prominent inhibitory effect of dasatinib was also observed in the ADCC test using Obinutuzumab (OBI), an anti-CD20 mAb engineered to increase the efficacy of ADCC (**Fig. 3E, right panel, Suppl. Fig. 6F**). In all ADCC tests presented above, imatinib and asciminib did not show any significant reduction in cytotoxicity, regardless of whether they were used with or without pre-incubation (**Fig. 3C, E, Suppl. Fig. 6B, D, and E**). Finally, we compared the effects of all tested TKIs on natural NK cell cytotoxicity without the addition of antibodies, using K562 as targets and NK cells isolated from healthy donors as effectors (**Fig. 3F**). We found that natural cytotoxicity was almost completely abolished in the presence of dasatinib in both tested doses, Cmax and ¼ Cmax, and partially reduced in the Cmax doses of ponatinib and bosutinib (**Fig. 3G, Suppl. Fig. 6G**). Neither imatinib nor asciminib influenced the natural cytotoxicity of NK cells (**Fig. 3G, Suppl. Fig. 6G**). In summary, these results demonstrate that TKIs have varying effects on ADCC mediated by anti-CD20 mAbs, with a significant reduction in cytotoxicity largely attributed to their impact on immune effector cells rather than CD20 downregulation on leukemic cells. Notably, asciminib and imatinib do not reduce the efficacy of ADCC mediated by anti-CD20 mAb in any of the settings tested.

Asciminib does not impair NK cell degranulation in an ex vivo assay

In previous experiments, we have shown that some TKIs, especially dasatinib, at concentrations achievable in serum after oral administration, can negatively affect the effector functions of NK cells. To further investigate the effects of TKIs on NK cell function, we performed a degranulation assay using primary NK cells isolated from healthy donors primed for degranulation with the K562 cells. Our findings demonstrate a complete suppression of NK cell degranulation following dasatinib treatment, while partial suppression following ponatinib exposure (**Figure 4A**). To

further verify our results, we tested the degranulation capacity of NK cells in blood collected from CML and Ph$^+$ BCP-ALL patients who received imatinib, dasatinib or asciminib. Blood samples were collected before drug administration, 1 hour, and 24 hours after oral administration of the standard dose of the TKI, and no additional TKI was added to the assay (**Figure 4B, left panel**). We observed inhibition of NK cell degranulation in all blood samples collected one hour or one day after administration of dasatinib (**Figure 4B, right panel**). In contrast, NK cell activity was not reduced in blood samples collected at 1 hour or 24 hours after administration of asciminib nor at 1 hour after administration of imatinib (**Figure 4B, right panel**). These *ex vivo* results confirm that asciminib and imatinib do not interfere with NK cell function at concentrations achievable in patients' blood, while dasatinib exhibits negative effects.

Asciminib does not interfere with RTX-mediated ADCP

Next, we investigated the effects of TKIs on ADCP, another immune effector mechanism relevant to the antitumor activity of RTX [27,30]. To assess the function of macrophages, we performed an *in vitro* phagocytosis assay using Ph$^+$ CD20$^+$ BCP-ALL PDXs as targets and human primary M1 macrophages differentiated from the primary human monocytes as effectors. RTX-opsonized targets and effectors were separately preincubated for 2 hour with two different concentrations of TKIs, and then mixed to enable ADCP for 1 hour (**Fig. 5A**). As shown in **Fig. 5B**, RTX-ADCP was reduced in presence of Cmax concentration of dasatinib in 4 out of 5 tested PDXs. Additionally, the reduction of ADCP was also observed in the presence of ponatinib and imatinib in two out of five PDXs. Asciminib at Cmax, but not ¼ Cmax reduced ADCP of one PDX tested (**Suppl. Fig. 7A**). In the pooled experimental data from all tested PDXs, we observed a reduction of RTX-ADCP when the assay was performed in the presence of Cmax or ¼ Cmax concentrations of imatinib, dasatinib, and ponatinib, however, this reached statistical significance only for imatinib and dasatinib (**Fig. 5C, Suppl. Fig. 7B**). These results indicate that dasatinib and imatinib block the engulfment of RTX-opsonized CD20$^+$ Ph$^+$ BCP-ALL PDX cells to the

greatest extent, ponatinib to a lesser extent, while asciminib does not significantly interfere with RTX-mediated ADCP.

In summary, although all tested TKIs decreased RTX-mediated CDC, their effects on effector cells differed, with asciminib exhibiting the most favorable profile. The summary of TKIs' effects on anti-CD20 mAb-mediated cytotoxicity is presented in Fig. 6.

Discussion

The incorporation of RTX into chemotherapy has markedly enhanced treatment outcomes in adult Ph$^-$ CD20$^+$ BCP-ALL patients[6], facilitating its inclusion in treatment protocols. Furthermore, an ongoing clinical trial will compare the efficacy of OBI against RTX in adult BCP-ALL patients (clinicaltrials.gov: NCT04920968). Preliminary trials also reveal the potential effectiveness of anti-CD20 therapy in pediatric cohorts, suggesting an opportunity for enlarging the pool of eligible patients[31,32]. Considering that anti-CD20 mAbs are commonly combined with other drugs, it is essential to analyze the reciprocal influences on efficacy. Our study reveals a frequent CD20 expression among Ph$^+$ BCP-ALL patients, inferring combined use of TKIs and RTX. TKIs play a critical role in the treatment of Ph$^+$ BCP-ALL and are administered in all phases of treatment. Imatinib and dasatinib serve as frontline therapies, while ponatinib is utilized in cases with detected T315I kinase domain mutation. Asciminib, an allosteric inhibitor, is not yet approved for Ph$^+$ BCP-ALL treatment. Our studies disclose substantial TKI-induced decreases in CD20 levels and interference of selected TKIs with critical effector cell functions, thereby potentially impacting treatment effectiveness in Ph$^+$ BCP-ALL patients and implying treatment refinements.

RTX is commonly used in adult BCP-ALL therapy worldwide, but its efficacy in the Ph$^+$ subgroup of CD20$^+$ BCP-ALL patients was mainly assessed in combination with imatinib[33,34]. A recent analysis of 118 adult patients in Mexico suggested a potential improvement in overall

survival (OS) among CD20^{+} patients treated with RTX and TKI (mostly imatinib)[33]. Additionally, a Korean Phase II multi-center study found RTX-containing regimens with imatinib to be superior in CD20^{+} Ph^{+} patients compared to historical groups without RTX[34]. There is a lack of clinical evaluation on the efficacy of other TKIs in combination with anti-CD20 mAbs. Although nowadays bispecific antibodies and adoptive cellular therapies are emerging treatments for relapsed and refractory BCP-ALL patients, their high costs limit accessibility in many countries. Therefore, RTX or its biosimilars could serve as cost-effective treatments for CD20^{+} Ph^{+} BCP-ALL potentially reducing disease relapse rates.

Our results suggest variability among TKIs in their suitability for combination with anti-CD20 antibodies. While all TKIs similarly downregulated CD20 levels in both BCP-ALL cell lines and PDXs and diminished RTX-mediated CDC, dasatinib also substantially inhibited NK cell cytotoxic activity and macrophage phagocytic function at various concentrations in both *in vitro* and *ex vivo* settings. We also noted inhibitory effects of ponatinib at Cmax concentrations on ADCC. These results correspond with existing literature pinpointing dasatinib and ponatinib inhibitory influence on NK cells and ADCC ascribed to their broader suppressive activity on critical SRC kinases[35,36]. Our investigations further underscore the adverse implications of dasatinib, and to a lesser degree, imatinib on macrophage phagocytic capabilities. To the best of our knowledge, this is the first report showing the effects of TKIs on human immunophagocytosis. Additional research is needed to delineate the precise mechanisms underlying these inhibitory effects. Contrary to other TKIs, asciminib did not compromise any effector cell-dependent mechanisms of cytotoxicity of anti-CD20 mAbs *in vitro*. This was confirmed by the stable NK cell degranulation observed in the blood of patients treated with asciminib. Given dasatinib's substantial negative impact on essential effector mechanisms pivotal for RTX efficacy, its potential to undermine antibody efficacy in patients is considerable. Consequently, TKI selection for combination with anti-CD20 mAbs warrants meticulous

consideration, with alternatives like asciminib potentially offering more potent combination strategies. Combining different generations of TKIs should also be considered, as combination of ponatinib with asciminib has shown promise in treating highly resistant CML and Ph[+] BCP-ALL[37 38].

The inhibitory effects of TKIs on cytotoxic effector cells were previously tested in the context of T-cell engaging bispecific antibodies, revealing a reduction in the antitumor efficacy of blinatumomab when used with dasatinib and ponatinib[39]. Despite these preclinical findings, recent clinical trials have shown promising therapeutic outcomes of dasatinib or ponatinib combined with blinatumomab[40,41], highlighting the limitations of preclinical studies in predicting clinical outcome. However, it is important to note significant differences in the mechanisms of antitumor activity between blinatumomab and rituximab. While blinatumomab targets tumor cells exclusively by engaging T cells via CD19-CD3 interaction, rituximab activates complement, NK cells, and macrophages after binding to CD20. In our study, we observed negative effects of dasatinib and, to a lesser extent, ponatinib on both diminishing the level of a target antigen CD20 and inhibiting various types of effector cells. Therefore, we firmly believe that our preclinical data could have implications for the clinical efficacy of combinations involving RTX.

Our research also underscores the potential importance of anti-CD20 mAbs selection in therapeutic strategies for Ph[+] BCP-ALL. Currently, only RTX, which functions via CDC, ADCC, and ADCP mechanisms[9,26], is employed in BCP-ALL treatment. Concurrently, OBI, primarily facilitating ADCC[10], is under clinical investigation. Our findings illustrate that all TKIs reduce CD20 mRNA, total protein, and cell surface protein levels in majority of BCP-ALL cell lines and PDXs. Notably, during the MRD assessment, we noted a subtle decline in CD20 levels in Ph[+] BCP-ALL blasts relative to diagnosis, a contrast to the elevation observed in the Ph[-] BCP-ALL patient group. Given that the principal distinction in the multi-drug combination therapy between Ph[+] and Ph[-] groups is the presence of a TKI (primarily imatinib) in the former group, it is

plausible that the noted CD20 reduction is linked to the inclusion of the TKI in the treatment protocol. It is pertinent to note that the reduction of CD20 by TKIs is possibly mediated by the on-target inhibition of BCR::ABL1, making it challenging to eliminate. Interestingly, this significant, albeit partial, CD20 reduction, does not negatively influence effector mechanisms aside from CDC. This aligns with previous studies indicating a specific dependency of CDC on CD20 levels, unlike ADCC, which maintains efficacy at reduced CD20 levels[29]. In light of these findings, our results hint at the potential superiority of OBI as an anti-CD20 mAb in conjunction with TKIs, especially those not adversely affecting ADCC, like imatinib or asciminib.

In summary, our study underscores the crucial role of precise TKI selection when used in combination with anti-CD20 mAbs for the treatment of CD20$^+$ Ph$^+$ BCP-ALL. Considering the downregulation of CD20 by all tested TKIs, the use of OBI, which potently eliminates CD20$^+$ cells independently of CDC, may be beneficial for CD20$^+$ Ph$^+$ BCP-ALL patients. In terms of TKI selection, we propose asciminib as a prime candidate for combination therapy, given its minimal impact on immune effector cell function. Our results may have a broader impact, given the ever-increasing use of immunotherapies involving immune effector cells, which are also being tested in clinical trials in combination with dasatinib and other TKIs[42].

References

1. Pui CH, Yang JJ, Hurgen SP, et al. Childhood Acute Lymphoblastic Leukemia: Progress Through Collaboration. J Clin Oncol. 2015; 33(27):2938-2948.

2. Lilljebjörn H, Fioretos T. New oncogenic subtypes in pediatric B-cell precursor acute lymphoblastic leukemia. Blood. 2017;130(12):1395-1401.

3. Tan FH, Putoczki TL, Stylli SS, Luwor RB. Ponatinib: a novel multi-tyrosine kinase inhibitor against human malignancies. OncoTargets Ther. 2019;12:635-645.

4. Monestime S, Al Sagheer T, Tadros M. Asciminib (Scemblix): A third-line treatment option for chronic myeloid leukemia in chronic phase with or without T315I mutation. Am J Health Syst Pharm. 2023;80(2):36-43.

5. Samra B, Jabbour E, Ravandi F, Kantarjian H, Short NJ. Evolving therapy of adult acute lymphoblastic leukemia: state-of-the-art treatment and future directions. J Hematol Oncol. 2020;13(1):70.

6. Maury S, Chevret S, Thomas X, et al. Rituximab in B-Lineage Adult Acute Lymphoblastic Leukemia. N Engl J Med. 2016;375(11):1044-1053.

7. National Comprehensive Cancer Network®; NCCN Clinical Practice Guidelines in Oncology (NCCN Guidelines®) Acute Lymphoblastic Leukemia Version 4.2023, ALL-D, 1 of 9 - https://www.nccn.org/professionals/physician_gls/pdf/all.pdf. Accessed May 13, 2024

8. National Comprehensive Cancer Network®; NCCN Clinical Practice Guidelines in Oncology (NCCN Guidelines®) Acute Lymphoblastic Leukemia Version 4.2023, MS-26 - https://www.nccn.org/professionals/physician_gls/pdf/all.pdf. Accessed May 13, 2024

9. Boross P, Leusen JHW. Mechanisms of action of CD20 antibodies. Am J Cancer Res. 2012;2(6):676-990.

10. Meyer S, Evers M, Jansen JHM, et al. New insights in Type I and II CD20 antibody mechanisms-of-action with a panel of novel CD20 antibodies. Br J Haematol. 2018;180(6):808-820.

11. Esteban RE, Christianne B, Alvaro A, Demichelis-Gómez R. Prognostic Effect of CD20 Expression in Adult B-cell Acute Lymphoblastic Leukemia. Clin Lymphoma Myeloma Leuk. 2018;18(5):361-367.

12. Thomas DA, O'Brien S, Jorgensen JL, et al. Prognostic significance of CD20 expression in adults with de novo precursor B-lineage acute lymphoblastic leukemia. Blood. 2009;113(25):6330-6337.

13. Jeha S, Behm F, Pei D, et al. Prognostic significance of CD20 expression in childhood B-cell precursor acute lymphoblastic leukemia. Blood. 2006;108(10):3302-3304.

14. Pavlasova G, Mraz M. The regulation and function of CD20: an "enigma" of B-cell biology and targeted therapy. Haematologica. 2020;105(6):1494-1506.

15. Alduailej H, Kanfar S, Bakhit K, et al. Outcome of CD20-positive Adult B-cell Acute Lymphoblastic Leukemia and the Impact of Rituximab Therapy. Clin Lymphoma Myeloma Leuk. 2020;20(9):e560-e568.

16. Dworzak MN, Schumich A, Printz D, et al. CD20 up-regulation in pediatric B-cell precursor acute lymphoblastic leukemia during induction treatment: setting the stage for anti-CD20 directed immunotherapy. Blood. 2008;112(10):3982-3988.

17. Serbanica AN, Popa DC, Caruntu C, et al. The Significance of CD20 Intensity Variance in Pediatric Patients with B-Cell Precursor Acute Lymphoblastic Leukemia. J Clin Med. 2023;12(4):1451.

18. Dworzak MN, Gaipa G, Schumich A, et al. Modulation of antigen expression in B-cell precursor acute lymphoblastic leukemia during induction therapy is partly transient: evidence for a drug-induced regulatory phenomenon. Results of the AIEOP-BFM-ALL-FLOW-MRD-Study Group. Cytometry B Clin Cytom. 2010;78(3):147-153.

19. Winiarska M, Bojarczuk K, Pyrzynska B, et al. Inhibitors of SRC kinases impair antitumor activity of anti-CD20 monoclonal antibodies. mAbs. 2014;6(5):1300-1313.

20. Schade AE, Schieven GL, Townsend R, et al. Dasatinib, a small-molecule protein tyrosine kinase inhibitor, inhibits T-cell activation and proliferation. Blood. 2008;111(3):1366-1377.

21. Krusch M, Salih HR. Effects of BCR-ABL inhibitors on anti-tumor immunity. Curr Med Chem. 2011;18(34):5174-5184.

22. Appel S, Balabanov S, Brümmendorf TH, Brossart P. Effects of imatinib on normal hematopoiesis and immune activation. Stem Cells. 2005;23(8):1082-1088.

23. Weichsel R, Dix C, Wooldridge L, et al. Profound inhibition of antigen-specific T-cell effector functions by dasatinib. Clin Cancer Res. 2008;14(8):2484-2491.

24. Urbańska Z, Lejman M, Taha J, et al. The kinetics of blast clearance are associated with copy number alterations in childhood B-cell acute lymphoblastic leukemia. Neoplasia. 2023;35:100840.

25. Bobrowicz M, Dwojak M, Pyrzynska B, et al. HDAC6 inhibition upregulates CD20 levels and increases the efficacy of anti-CD20 monoclonal antibodies. Blood. 2017;130(14):1628-1638.

26. Winiarska M, Glodkowska-Mrowka E, Bil J, Golab J. Molecular mechanisms of the antitumor effects of anti-CD20 antibodies. Front Biosci (Landmark Ed). 2011;16(1):277-306.

27. Church AK, VanDerMeid KR, Baig NA, et al. Anti-CD20 monoclonal antibody-dependent phagocytosis of chronic lymphocytic leukaemia cells by autologous macrophages. Clin Exp Immunol. 2016;183(1):90-101.

28. Golay J, Lazzari M, Facchinetti V, et al. CD20 levels determine the in vitro susceptibility to rituximab and complement of B-cell chronic lymphocytic leukemia: further regulation by CD55 and CD59. Blood. 2001;98(12):3383-3389.

29. van Meerten T, van Rijn RS, Hol S, Hagenbeek A, Ebeling SB. Complement-induced cell death by rituximab depends on CD20 expression level and acts complementary to antibody-dependent cellular cytotoxicity. Clin Cancer Res. 2006;12(13):4027-4035.

30. Oflazoglu E, Audoly LP. Evolution of anti-CD20 monoclonal antibody therapeutics in oncology. mAbs. 2010;2(1):14-19.

31. Attias D, Weitzman S. The efficacy of rituximab in high-grade pediatric B-cell lymphoma/leukemia: a review of available evidence. Curr Opin Pediatr. 2008;20(1):17-22.

32. Gupta AK, Chopra A, Meena JP, et al. Rituximab added to standard chemotherapy and its effect on minimal residual disease during induction in CD20 positive pediatric acute lymphoblastic leukemia: a pilot RCT. Am J Blood Res. 2021;11(6):571-579.

33. Rodriguez-Rodriguez S, Rios Olais FA, Mora A, et al. The Impact of Adding Rituximab to the Standard Chemotherapy + TKI Regimen in Adults with Philadelphia-Positive B Acute Lymphoblastic Leukemia: A Multicenter Retrospective Study. Blood. 2023;142(Supplement 1):4204.

34. Baek DW, Park HS, Sohn SK, et al. Rituximab plus multiagent chemotherapy for newly diagnosed CD20-positive acute lymphoblastic leukemia: a prospective phase II study. Korean J Intern Med. 2023;38(5):734-746.

35. Gushwa NN, Kang S, Chen J, Taunton J. Selective targeting of distinct active site nucleophiles by irreversible SRC-family kinase inhibitors. J Am Chem Soc. 2012;134(50):20214-20217.

36. Montero JC, Seoane S, Ocaña A, Pandiella A. Inhibition of SRC family kinases and receptor tyrosine kinases by dasatinib: possible combinations in solid tumors. Clin Cancer Res. 2011;17(17):5546-5552.

37. Eide CA, Zabriskie MS, Savage Stevens SL, et al. Combining the Allosteric Inhibitor Asciminib with Ponatinib Suppresses Emergence of and Restores Efficacy Against Highly Resistant BCR-ABL1 Mutants. Cancer Cell. 2019;36(4):431-443.e5.

38. Zerbit J, Tamburini J, Goldwirt L, et al. Asciminib and ponatinib combination in Philadelphia chromosome-positive acute lymphoblastic leukemia. Leuk Lymphoma. 2021;62(14):3558-3560.

39. Leonard JT, Kosaka Y, Malla P, et al. Concomitant use of a dual Src/ABL kinase inhibitor eliminates the in vitro efficacy of blinatumomab against Ph+ ALL. Blood. 2021;137(7):939-944.

40. Jabbour E, Short NJ, Jain N, et al. Ponatinib and blinatumomab for Philadelphia chromosome-positive acute lymphoblastic leukaemia: a US, single-centre, single-arm, phase 2 trial. Lancet Haematol. 2023;10(1):e24-34.

41. Foà R, Bassan R, Vitale A, et al. Dasatinib-Blinatumomab for Ph-Positive Acute Lymphoblastic Leukemia in Adults. N Engl J Med. 2020;383(17):1613-1623.

42. Saleh K, Fernandez A, Pasquier F. Treatment of Philadelphia Chromosome-Positive Acute Lymphoblastic Leukemia in Adults. Cancers (Basel). 2022;14(7):1805.

Figure legends

Figure 1. Philadelphia-positive B-cell precursor acute lymphoblastic leukemia (Ph⁺ BCP-ALL) blasts more frequently show CD20 positivity.

A. The median levels of *MS4A1* mRNA relative to *B2M* housekeeping gene were determined by RT-qPCR in bone marrow-derived BCP-ALL cells isolated from pediatric and adult BCP-ALL patients (n=130), representing defined genetic subtypes of the disease. Each dot corresponds to an individual sample. *P* values were calculated using the Kruskal-Wallis test followed by Dunn's multiple comparisons. *$*P<0.05$, $***P<0.001$.*

B. The levels of surface CD20 were assessed by flow cytometry in BCP-ALL cells obtained from pediatric and adult Ph⁺ (n=35) and Ph⁻ (n=120) BCP-ALL patients at diagnosis, and the median percentage of CD20⁺ cells was calculated for each group. The clinical threshold of rituximab inclusion in BCP-ALL treatment protocol at 20% CD20⁺ blasts is displayed as a blue line. *P* values were calculated using the Mann-Whitney test, *$*P<0.05$.*

C. Diagrams showing the percentages of CD20-positive and CD20-negative patients in Ph⁺ and Ph⁻ subgroups of BCP-ALL, assessed for the same cohort as described in B. Patients with at least 20% CD20⁺ lymphoblasts are considered CD20-positive.

Figure 2. TKIs downregulate CD20 in Philadelphia-positive B-cell precursor acute lymphoblastic leukemia (Ph⁺ BCP-ALL) cells.

A. Surface CD20 median levels were assessed in primary samples obtained from pediatric BCP-ALL patients (n=130) at the time of diagnosis and during the assessment of the measurable residual disease (MRD), on day 15 after starting induction therapy (MRD15). Patients were treated according to the modified AIEOP-BFM 2017 or EsPhALL2017/COG AALL1631 protocol containing two weeks of exposure to steroids (dexamethasone, DEX, or prednisone, PRED),

one dose of L-asparaginase (LASP), one dose of vincristine (VCR), one dose of daunorubicin (DNR), as well as one intrathecal injection of methotrexate (MTX). Ph$^+$ BCP-ALL patients additionally received 0-3 doses of imatinib (IMAT). *P* value was calculated using the Wilcoxon matched-pairs signed-rank test, ****P*<0.001.

B. The differences in median CD20 levels at diagnosis and at MRD15 assessment were compared separately for Ph$^+$ (n=24) and Ph$^-$ (n=106) pediatric patients. P-value was calculated using the Wilcoxon matched-pairs rank test, ****P*<0.001.

C. Ph$^+$ BCP-ALL cell lines and Patient-Derived Xenograft (PDX) cells were incubated with Cmax concentrations of TKIs *in vitro* for 48 h. After treatment, the CD20 expression levels were determined by flow cytometry using an anti-CD20 antibody. Heatmap presents the log fold change of the CD20 fluorescence intensity levels (geomean) in drug-treated cells relative to untreated controls.

D. BV173 cells were incubated with TKIs at Cmax concentrations for 24 h followed by RNA isolation and qPCR analysis. The graph shows the mean mRNA levels of the *MS4A1* relative to reference genes *(RPL29, GUSB)* from three independent experiments. *P* value was calculated using a one-way ANOVA test followed by Dunnett's test for multiple comparisons, ****P*<0.001.

 E. Ph$^+$ BCP-ALL cell lines were incubated for 48 h with drugs commonly used in Ph$^+$ BCP-ALL chemotherapy protocols. The concentrations of the drugs were determined by cytotoxicity tests and selected to be EC50 or Cmax, if the EC50 was not achieved. Detailed concentrations of drugs are described in Supplementary materials. Changes in the levels of CD20 were assessed and presented as described in C.

Figure 3. Effects of TKIs on Antibody-Dependent Cellular Cytotoxicity (ADCC) and Complement-Dependent Cytotoxicity (CDC) mediated by anti-CD20 mAbs.

A. Experimental scheme of the preincubation experiments. BV173 target cells were preincubated with Cmax concentrations of TKIs or DMSO (control) for 48 h. To assess CDC, target cells were incubated with human serum and rituximab (RTX) for 1h. To assess ADCC, the preincubated and CFSE-stained target cells were incubated for 4 h with CD16$^+$ NK92 cells RTX, and Cmax concentrations of TKIs or DMSO (control). The percentage of dead cells was assessed by flow cytometry.

B. After 48 h incubation with Cmax concentration of TKIs, BV173 cells were incubated with human serum and 20 µg/mL RTX. Next, dead cells were stained using propidium iodide (PI) and assessed in flow cytometry. Background cytotoxicity (dead cells in the group with serum, but without RTX) was deducted from the corresponding groups. The presented data are the means +/- SEM from at least four independent repeats.

C. After 48 h incubation with Cmax concentration of TKIs, CFSE-stained BV173 cells were incubated for 4 h with CD16$^+$ NK92 cells in effector:target ratio of 2.5:1, 10 µg/mL RTX, and Cmax concentrations of TKIs or DMSO (control). Upon incubation cells were stained with 7AAD and assessed by flow cytometry as the percentage of CFSE and 7AAD double-positive cells. The presented data are the means +/- SEM from at least four independent repeats.

D. Experimental plan without preincubation of BCP-ALL cells with TKIs. CFSE-stained BCP-ALL cells were incubated for 4 h with effector cells, anti-CD20 mAbs, and Cmax concentrations of TKIs or DMSO (control) and BCP-ALL cells' viability was assessed by flow cytometry.

E. CFSE-stained BV173 target cells were incubated for 4 h with CD16$^+$ NK92 cells in effector:target ratio of 2.5:1, Cmax concentrations of TKIs and 10 µg/mL RTX (left panel) or 10

µg/mL obinutuzumab (OBI) (right panel). The presented data are the means +/- SEM of at least three independent experiments. The percentages of dead cells were assessed as described in C.

F. Experimental scheme of the natural cytotoxicity experiments. NK cells were isolated from healthy donors and incubated with TKIs and CFSE-stained K562 target cells in effector:target ratio of 10:1 for 4 h without the addition of antibodies. The percentage of dead cells was assessed by flow cytometry as the percentage of CFSE and PI double-positive cells.

G. After 4 h incubation with NK cells and Cmax concentrations of TKIs, K562 cells were stained with propidium iodide and analyzed by flow cytometry as described in **F.**

The differences between groups in **B, C, E** and **G** were assessed by one-Way ANOVA with Dunnett's post hoc test, *P<0.05, **P<0.01, ***P<0.001.

Figure 4. Effects of TKIs on degranulation of NK cells *in vitro* and *ex vivo*.

A. NK cells isolated from healthy donors were incubated for 4 h with K562 cells and with Cmax concentrations of TKIs in effector:target ratio of 1:1. Degranulation was evaluated with flow cytometry as the percentage of CD107a$^+$ NK cells, with background (NK cell without targets) deducted. *P* values were calculated using one-way ANOVA test followed by Dunnett's multiple comparisons test, ****P*<0.001.

B. Left panel - experimental scheme of the whole blood *ex vivo* assay for testing the degranulation of NK cells. The blood was collected before (0 h), 1 h, and 24 h after oral administration of TKIs to Philadelphia-positive B-cell Precursor Acute Lymphoblastic Leukemia (Ph$^+$ BCP-ALL) or Chronic Myelogenous Leukemia (CML) patients. 150 µL of whole blood was then co-incubated with 400,000 K562 target cells for 4 h. Degranulation was evaluated with flow cytometry as the percentage of CD107a$^+$ NK cells after subtraction of background - samples with blood but without K562 target cells. Right panel - after 4 h incubation with K562 cells and red blood cell lysis, patients' cells were stained and analyzed by flow cytometry as described above. Patients underwent initial therapy (first dose) with specific TKIs in the case of dasatinib and asciminib, while those prescribed imatinib received subsequent doses in the regimen.

Figure 5. Effects of TKIs on RTX-mediated Antibody-Dependent Cellular Phagocytosis (ADCP).

A. Experimental scheme for ADCP assay (described in detail in the *Methods* section). Briefly, primary CD20$^+$ B-cell Precursor Acute Lymphoblastic Leukemia (BCP-ALL) Patient-Derived Xenograft (PDX) cells were stained with CFSE and opsonized with 5 µg/ml rituximab (RTX). Next, the PDX cells as well as primary human M1 macrophages were separately preincubated for 2 h with Cmax concentrations of TKIs and then co-incubated for 1 h in the presence of Cmax concentrations of TKIs. The percentage of phagocytosis was assessed by flow cytometry, as the

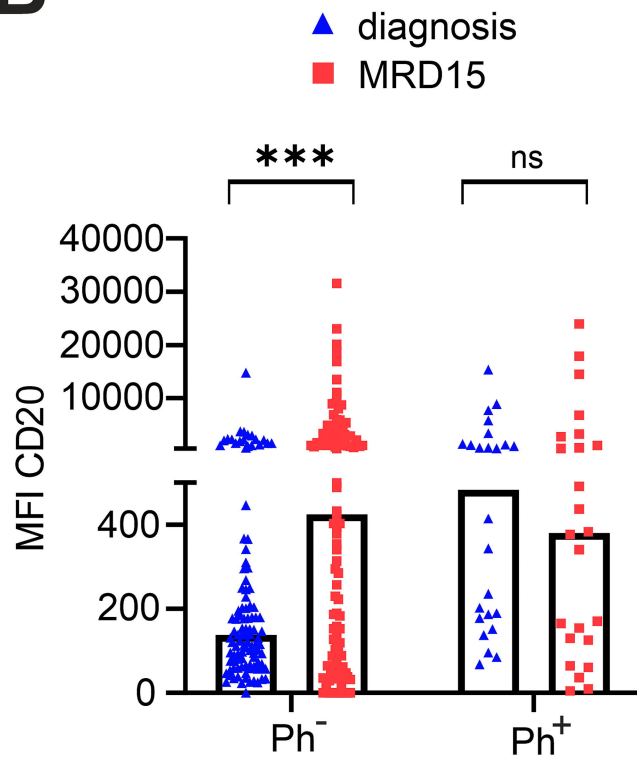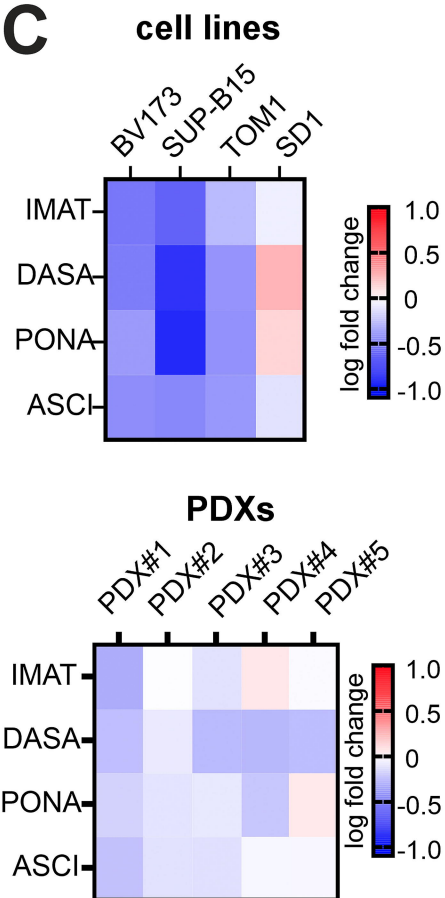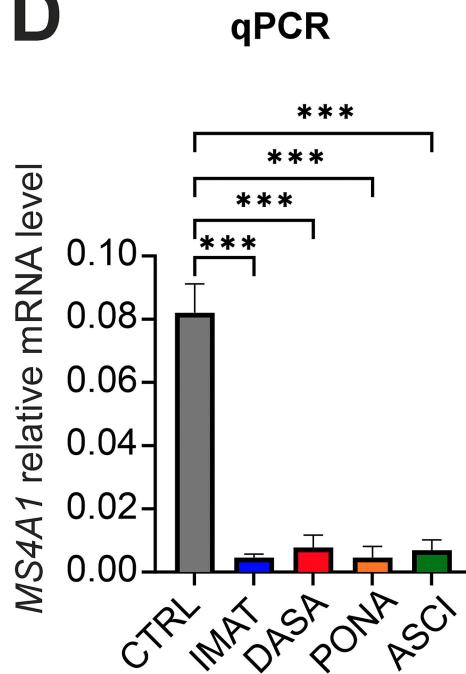fraction of double-positive macrophages. The background phagocytosis was assessed using cetuximab.

B. After background subtraction, phagocytosis was normalized to the highest technical replicate per donor. *P* values were calculated using a one-way ANOVA test followed by Dunnett's test for multiple comparisons, *$P<0.05$.
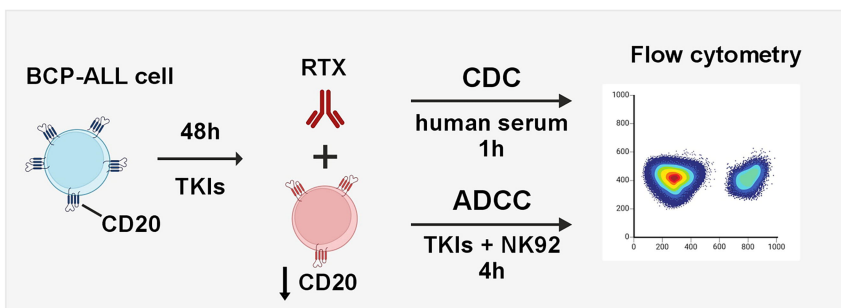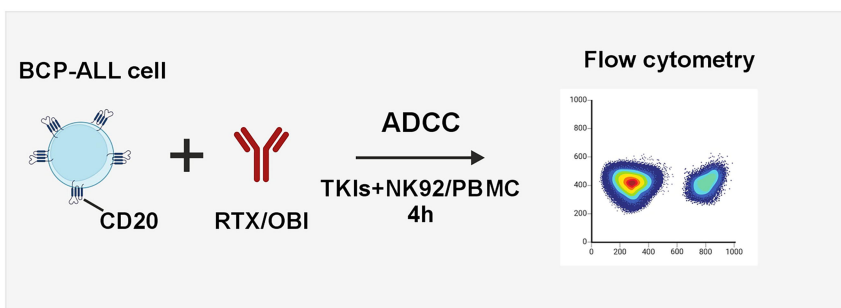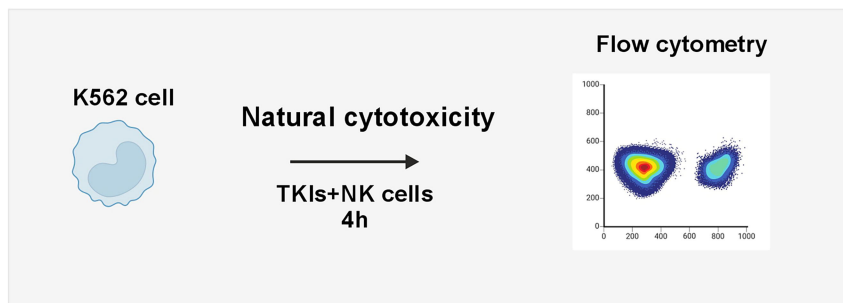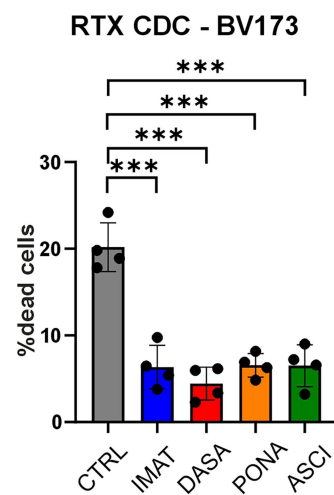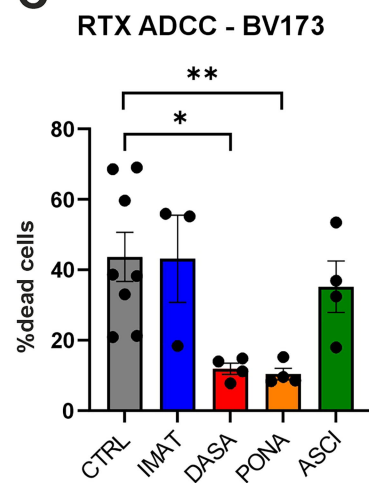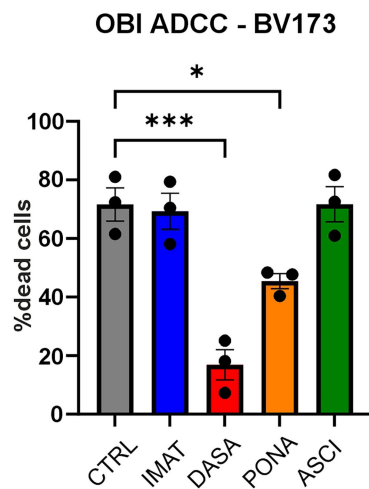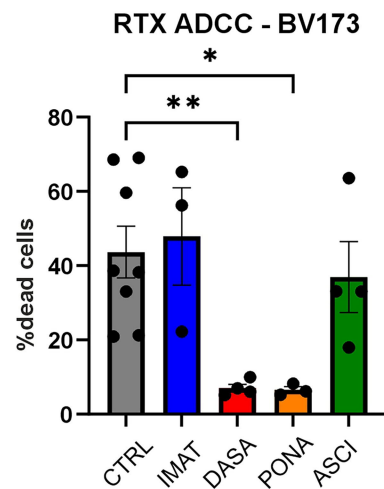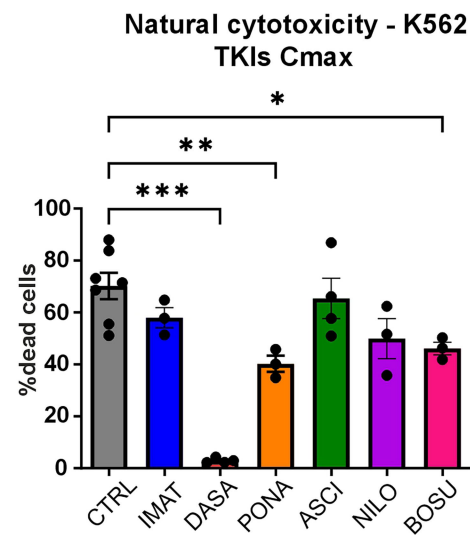
C. Summarized results of experiments from Figure **B** (n=5 PDXs). *P* values were calculated using Welch's ANOVA test followed by Dunnett's T3 test for multiple comparisons, ***$P<0.001$. A detailed description of the experimental setup can be found in Supplementary Methods.

**Figure 6. A summary of effects of TKIs in the different functional assays.**

The table presents a comparison of four TKIs, summarizing the results from figures 3-5, indicating whether antitumor efficacy is reduced or maintained in each functional assay. CDC – Complement-Dependent Cytotoxicity; ADCC – Antibody-Dependent Cellular Cytotoxicity; ADCP – Antibody-Dependent Cellular Phagocytosis.

A qPCR

B Flow cytometry
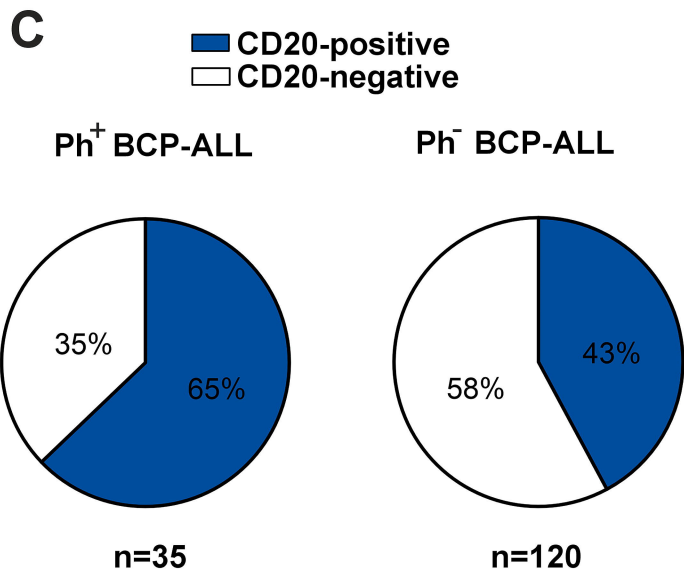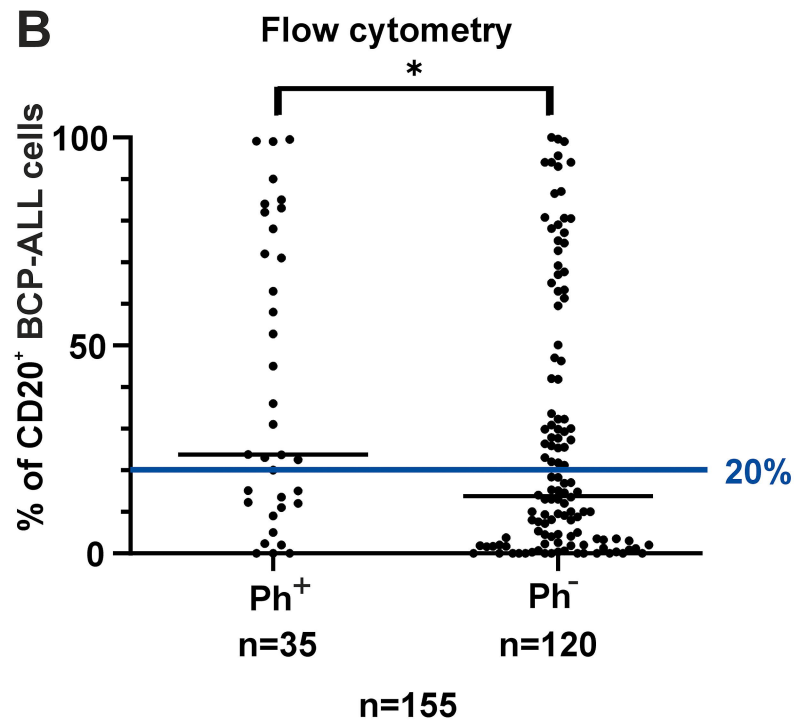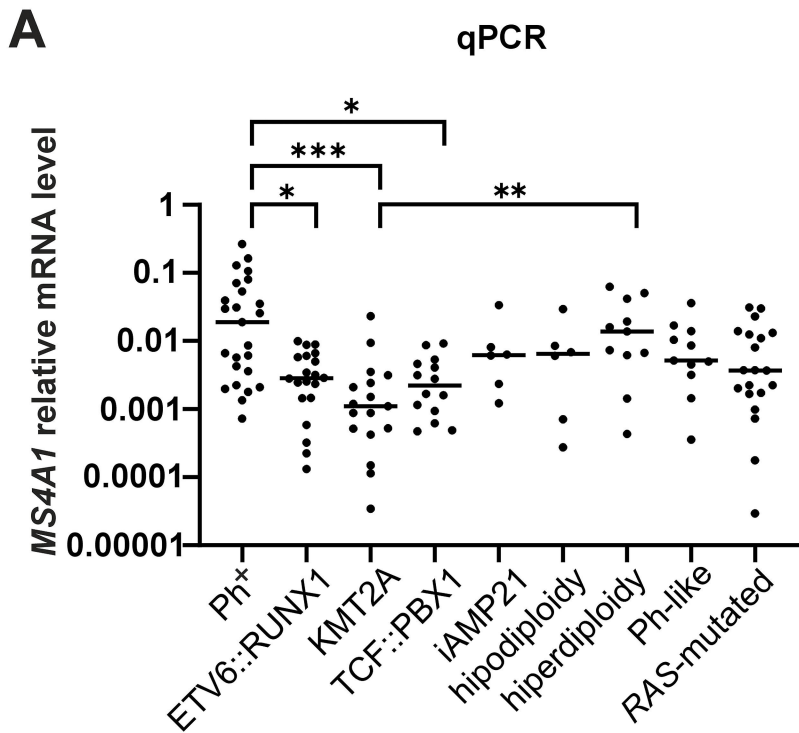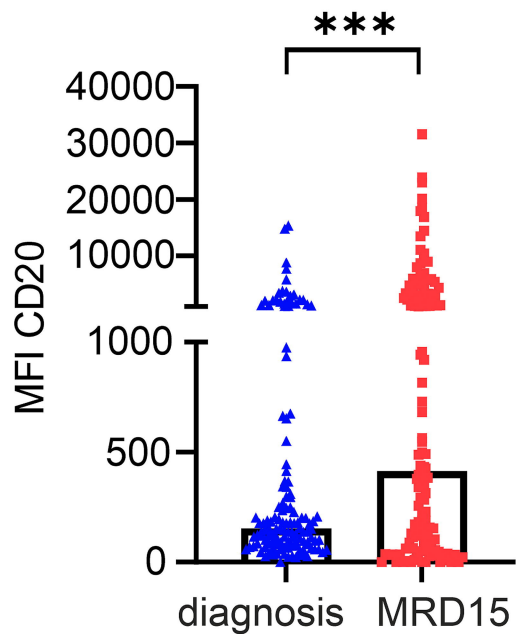
C
■ CD20-positive
□ CD20-negative
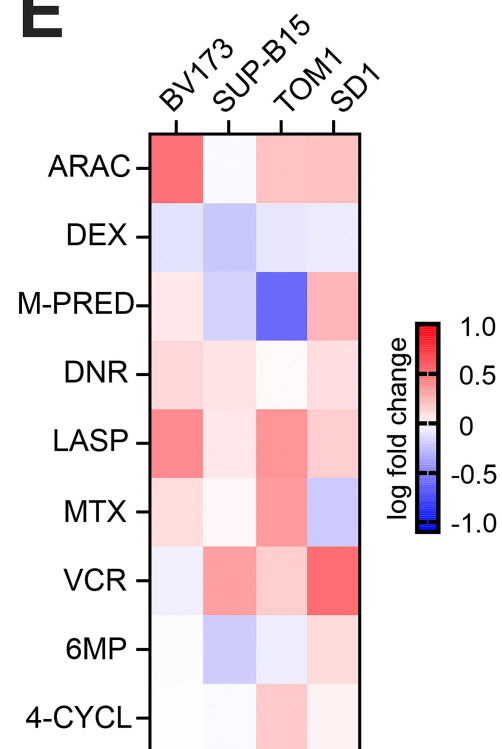
A BCP-ALL cell preincubation with TKIs - CDC and ADCC

B RTX CDC - BV173

C RTX ADCC - BV173

D No preincubation with TKIs - ADCC

E RTX ADCC - BV173   OBI ADCC - BV173

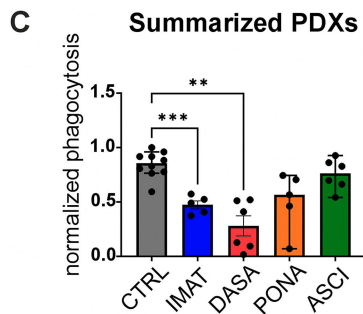**F** No preincubation with TKIs - Natural cytotoxicity

G Natural cytotoxicity - K562
TKIs Cmax

A NK cell degranulation *in vitro*
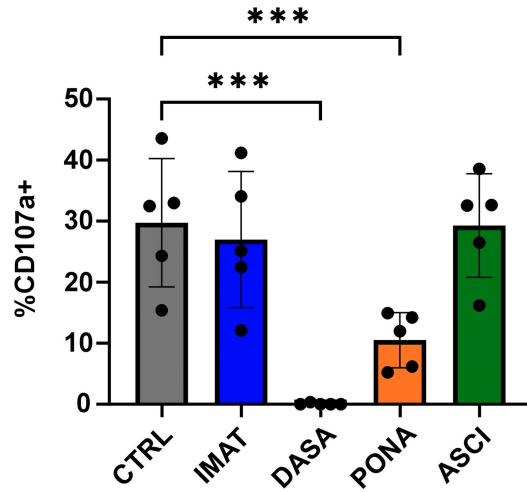
B NK cell degranulation *ex vivo* after oral administration of TKIs

A ADCP scheme

B

PDX#1 PDX#2 PDX#3 PDX#6 PDX#7

C Summarized PDXs
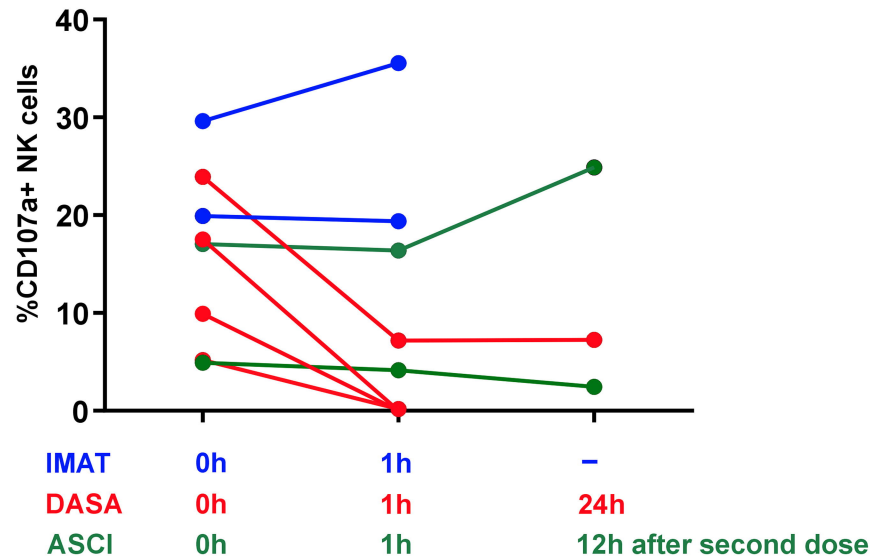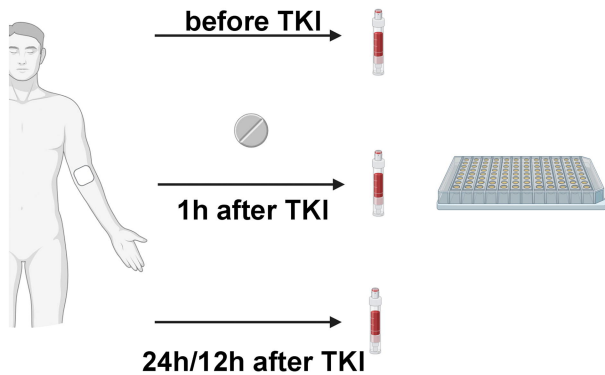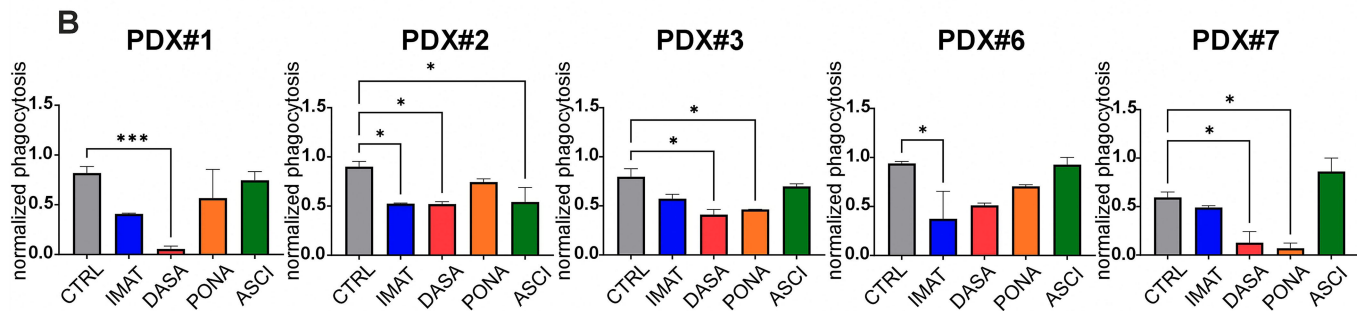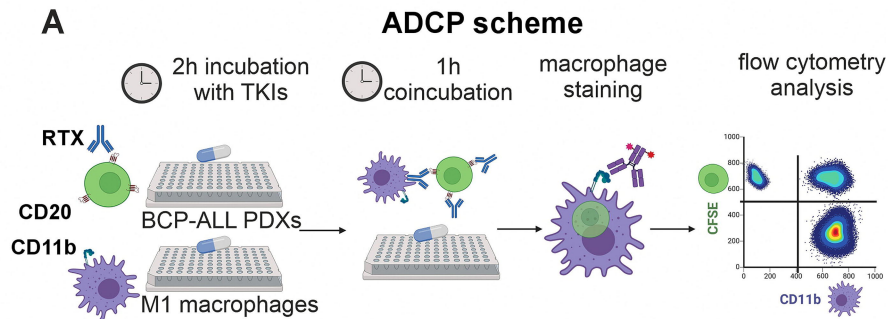
Functional assays in the presence of TKIs

	CDC	ADCC	Natural cytotoxicity	ADCP
IMAT	✗	✔	✔	✗
DASA	✗	✗	✗	✗
PONA	✗	✗	✗	✔
ASCI	✗	✔	✔	✔

Legend

anti-CD20 mAb

✗ antitumor effect decreased

✔ antitumor effect sustained

Supplementary material

Asciminib stands out as the superior tyrosine kinase inhibitor to combine with anti-CD20 monoclonal antibodies for the treatment of CD20+ Philadelphia-positive B-cell precursor acute lymphoblastic leukemia in preclinical models

Krzysztof Domka[1,2], Agnieszka Dąbkowska[1,2], Martyna Janowska[1], Zuzanna Urbańska[3,4], Agata Pastorczak[3,4], Magdalena Winiarska[1,2], Klaudyna Fidyt[2], Mieszko Lachota[5,6], Elżbieta Patkowska[7], Łukasz Sędek[8], Bartosz Perkowski[8], Jaromir Hunia[2], Justyna Jakubowska[3], Beata Krzymieniewska[7], Ewa Lech-Marańda[7], Wojciech Młynarski[3], Tomasz Szczepański[8], Małgorzata Firczuk[1,2]

[1]Laboratory of Immunology, Mossakowski Medical Research Institute Polish Academy of Sciences, Warsaw, Poland
[2]Department of Immunology, Medical University of Warsaw, Warsaw, Poland
[3]Department of Pediatrics, Oncology and Hematology, Medical University of Lodz, Lodz, Poland
[4] Department of Genetic Predisposition to Cancer, Medical University of Lodz, Lodz, Poland
[5]Laboratory of Cellular and Genetic Therapies, Medical University of Warsaw, Warsaw, Poland
[6]Department of Ophthalmology, Children's Memorial Health Institute, Warsaw, Poland
[7]Department of Hematology, Institute of Hematology and Transfusion Medicine, Warsaw, Poland
[8]Department of Pediatric Hematology and Oncology, Zabrze, Medical University of Silesia, Katowice, Poland

Supplementary figures

A

Correlation between CD20 MFI and *MS4A1* mRNA levels
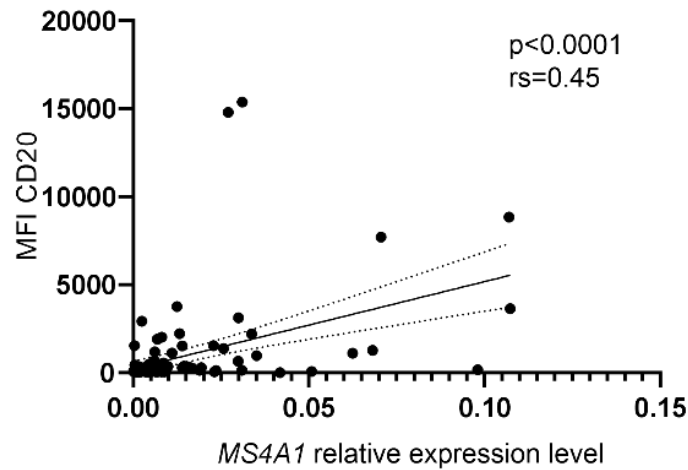
B

CD20-high BCP-ALL patients
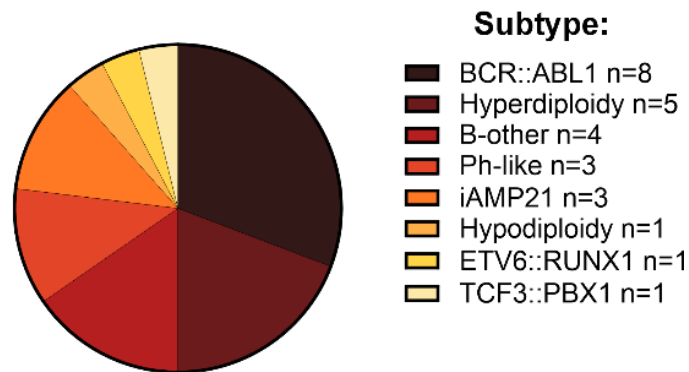
Total=26

Supplementary figure 1.

A. The Spearman correlation between *MS4A1* mRNA levels assessed by qPCR and CD20 surface protein levels assessed by flow cytometry (MFI) in the BCP-ALL primary samples (n=117 pediatric BCP-ALL patients) was analyzed using GraphPad Prism software.

B. Representation of genetic subtypes among CD20-high BCP-ALL pediatric patients. Patients with CD20 levels assessed by flow cytometry exceeding the MFI of 400 (22% of patients with the highest CD20 levels, n=26) were classified as CD20-high (BCR::ABL1 n=8, hyperdiploidy n=5, B-other n=4, Ph-like n=3, iAMP21 n=3, hypodiploidy n=1, ETV6::RUNX n=1, TCF::PBX1 n=1).
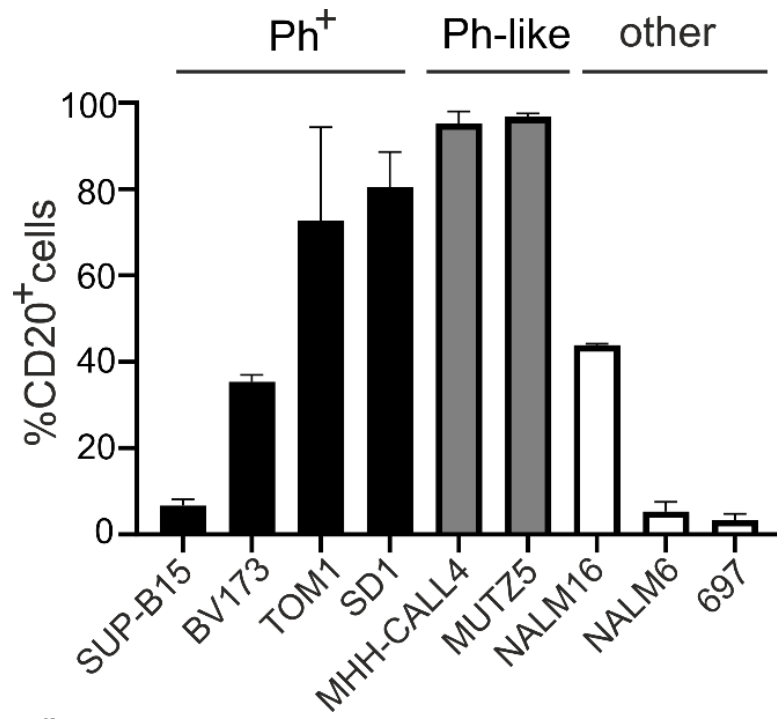
Supplementary figure 2.

Levels of surface CD20 were assessed in untreated BCP-ALL cell lines using flow cytometry. Mean percentages form 3 or 4 independent measurements are shown.

A

Ph$^+$

p = 0.75

Ph$^-$

*

B

Ph$^+$

p = 0.625

Ph$^-$

*
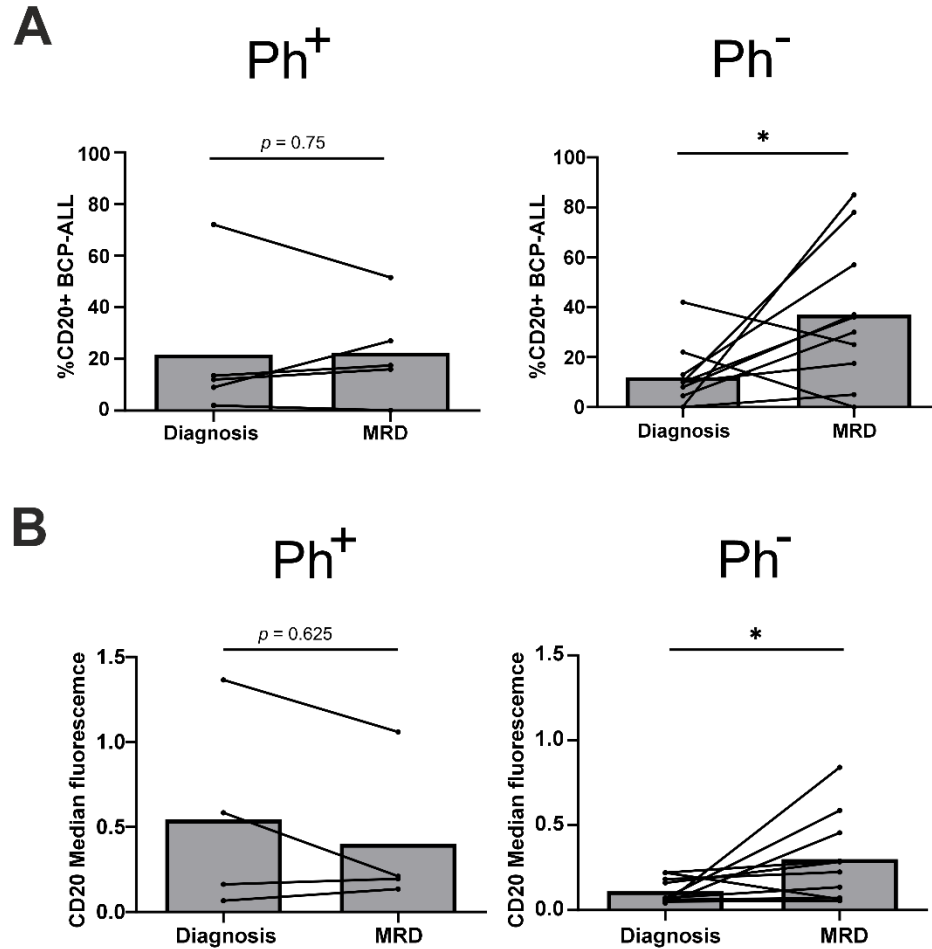
Supplementary figure 3. Changes in CD20 expression during treatment of adult BCP-ALL patients

Flow cytometry was employed to evaluate the percentages of CD20$^+$ BCP-ALL cells (**A**) and the median CD20 levels in BCP-ALL cells (**B**) in primary samples from adult BCP-ALL patients (n=15). These assessments were conducted at the time of diagnosis and during the measurable residual disease (MRD) evaluation specifically between 50 to 85 days after the initiation of induction therapy. Patients underwent treatment based on the Polish Adult Leukaemia Group (PALG) protocols PALG ALL6 or PALG ALL7. The supplementary methods provide a comprehensive list of drugs incorporated into the treatment protocols. Exclusion criteria for patients undergoing PALG ALL7 included those with 20% or more CD20$^+$ BCP-ALL cells, as these patients received RTX and the cells expressing CD20 were eliminated, as reported in [1]. *P* values were calculated using the Wilcoxon matched-pairs signed-rank test.

A

BV173

SUP-B15

TOM1

SD1

B

PDX#1

PDX#2

PDX#3

PDX#4

PDX#5
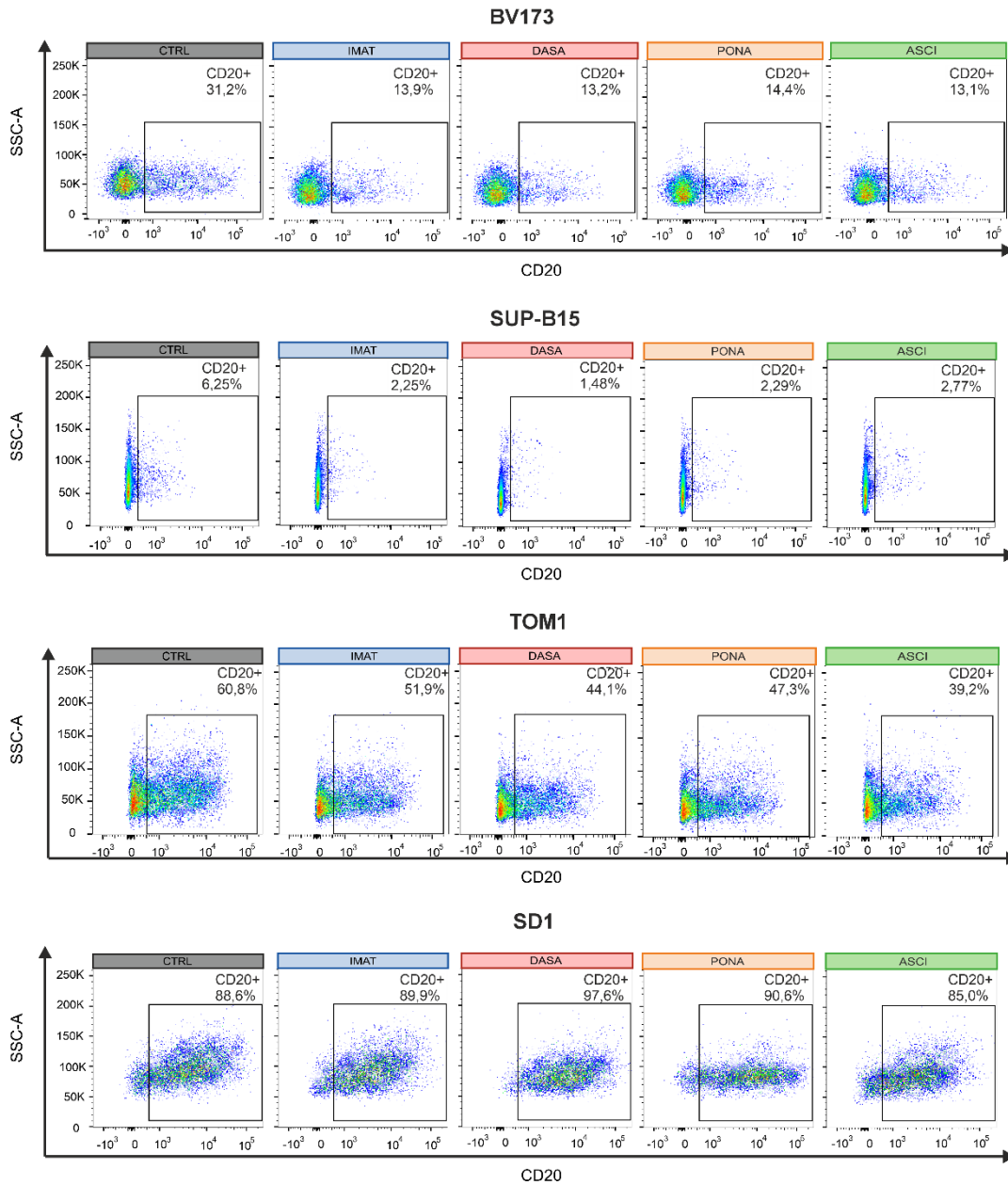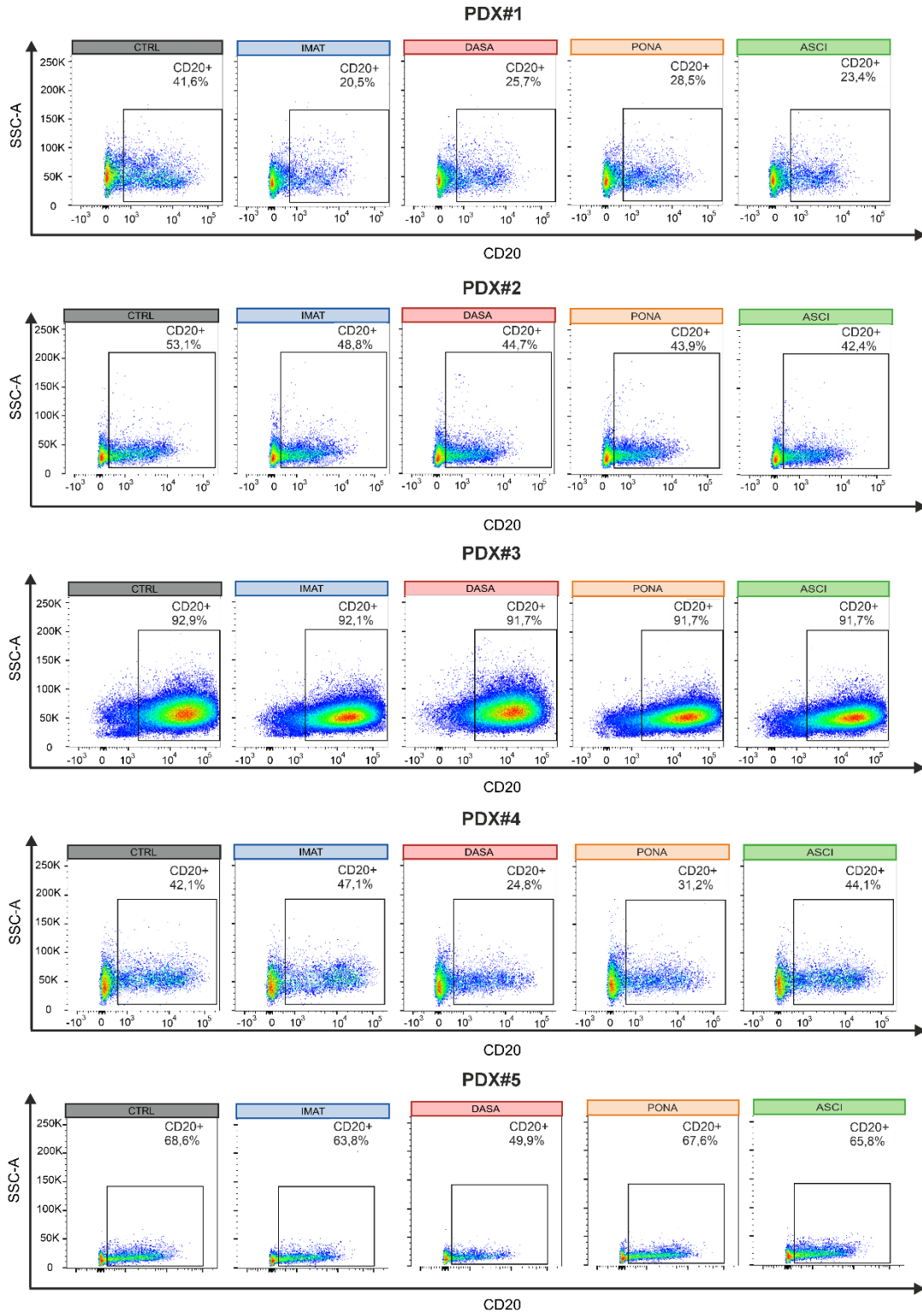
C
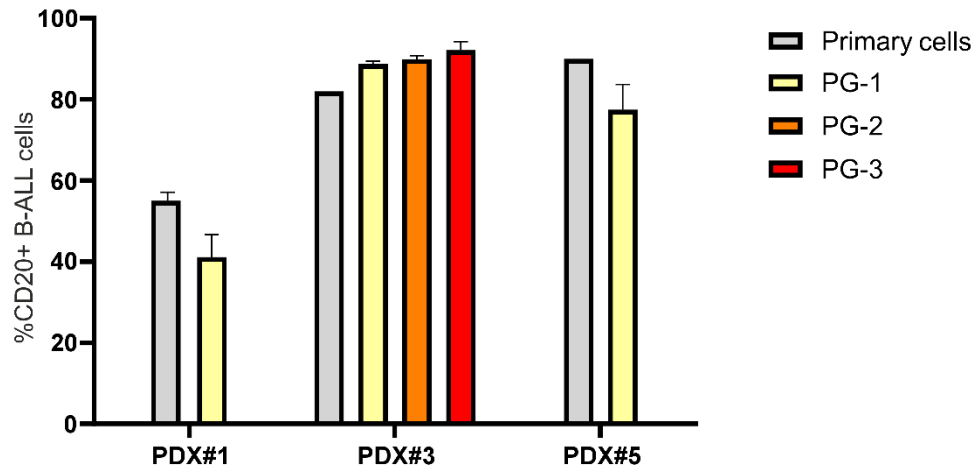
Supplementary figure 4. TKIs-mediated downregulation of CD20 on BCP-ALL cell lines and PDXs.

A., B. Ph[+] BCP-ALL cell lines (**A**) and PDXs (**B**) were incubated for 48 h with Cmax concentrations of TKIs *in vitro* for 48 h. After treatment, the CD20 surface protein levels on live cells were determined by flow cytometry using anti-CD20 antibody. Representative dot plots are shown.

C. Comparison of the percentage of CD20^{+} BCP-ALL cells between primary and PDX cells. The percentage of CD20^{+} BCP-ALL cells was determined by flow cytometry using anti-CD20 antibody. The first measurement was performed in primary cells at the time of the diagnostic assessment. The next measurements were performed after the first and subsequent generations of PDX cells in NSG mice.

BV173

48h
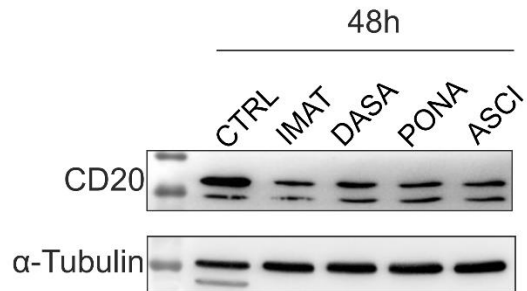
Supplementary figure 5. TKI-mediated downregulation of CD20 protein.

BV173 cells were exposed to Cmax concentrations of TKIs for 48 h. The levels of CD20 protein were determined by immunoblotting. The image shows representative blots of four independent experiments.

A PDX#2

B RTX ADCC - BV173
preincubated with TKIs
1/4 Cmax

C BV173   TOM1   PDX#2

D RTX ADCC - BV173
no preincubation with TKIs
1/4 Cmax

E RTX ADCC - SD1
Cmax   1/4 Cmax

F BV173 - OBI ADCC
1/4 Cmax

G Natural cytotoxicity - K562
TKIs 1/4 Cmax
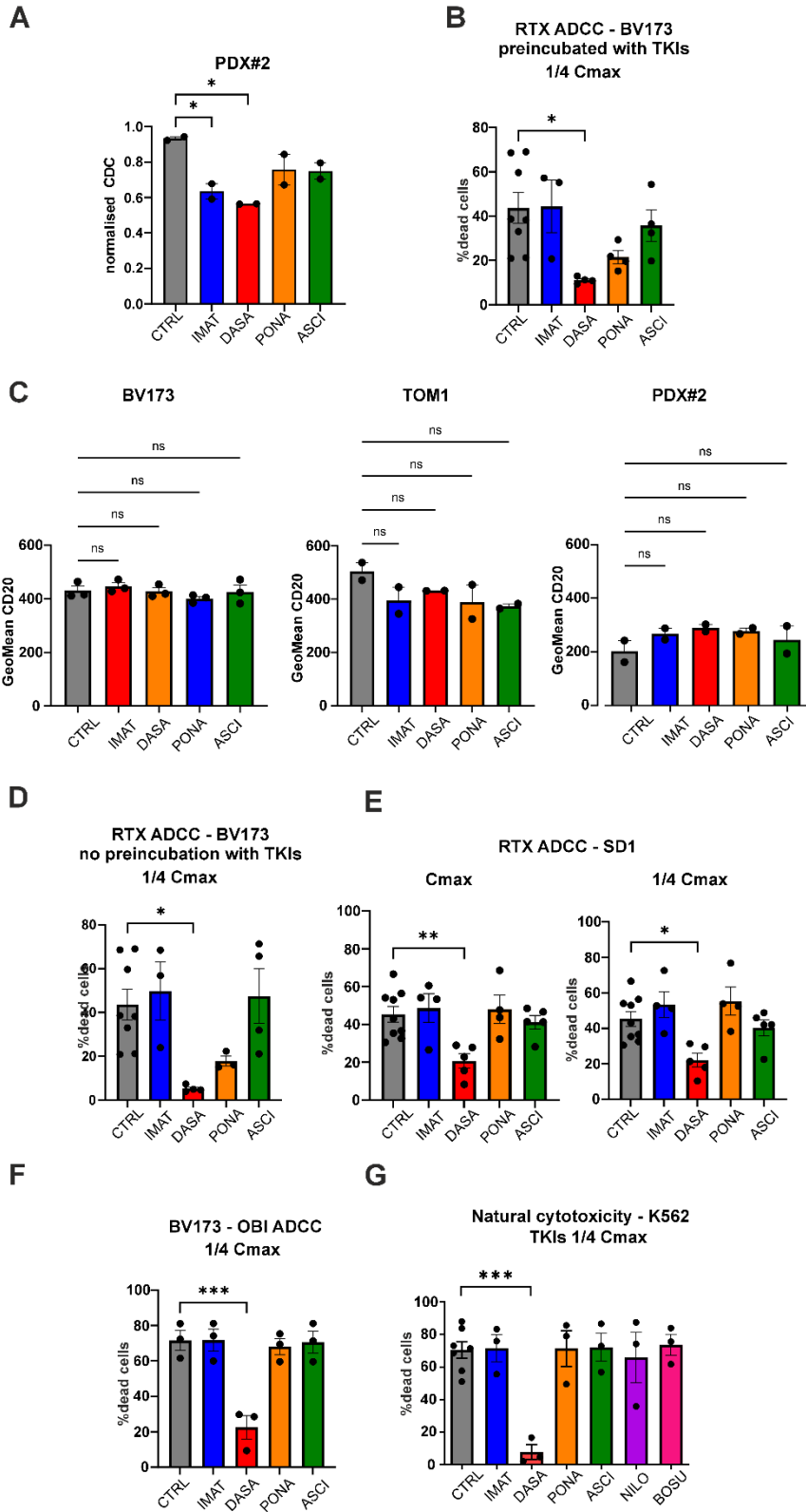
Supplementary figure 6. Effects of TKIs on CDC and ADCC mediated by anti-CD20 mAbs and the levels of CD20 in BCP-ALL cells.

A. PDX#2 BCP-ALL cells (target cells) were preincubated with Cmax concentrations of TKIs or DMSO (control) for 48 h. Next, the target cells were incubated with human serum and 20 µg/mL RTX for 1 h. Upon incubation, dead cells were stained with PI and the cytotoxicity was assessed by flow cytometry as % of PI-positive single cells. CDC was normalized to the highest technical replicate per experiment. The presented data are the means +/- SEM from two independent repeats.

B. CFSE-stained BV173 target cells were either preincubated with ¼ Cmax concentrations of TKIs or DMSO (control) for 48 h. Next, the target cells were incubated for 4 h with CD16+ NK92 cells in the effector:target ratio of 2.5:1, 10 µg/mL RTX, and ¼ Cmax concentrations of TKIs or DMSO (control). Dead target cells were stained with 7AAD and assessed in flow cytometry as the percentage of CFSE and 7AAD double-positive cells. The presented data are the means +/- SEM from at least three independent repeats.

C. Ph+ BCP-ALL cell lines and PDXs were incubated with Cmax concentrations of TKIs *in vitro* for 4 h. After treatment, the CD20 expression levels were determined by flow cytometry using an anti-CD20 antibody. The presented data are the means +/- SEM from at least two independent repeats.

D. CFSE-stained BV173 target cells were incubated for 4 h with CD16+ NK92 cells in effector:target ratio of 2.5:1, 10 µg/mL RTX and ¼ Cmax concentrations of TKIs. The presented data are the means +/- SEM of at least three independent experiments. The percentages of dead cells were assessed as described in **B.**

E. CFSE-stained SD1 target cells were incubated for 4 h with healthy donors' PBMCs in effector:target ratio of 25:1, 10 µg/mL RTX and Cmax (left panel) or ¼ Cmax (right panel) concentrations of TKIs. The presented data are the means +/- SEM of independent experiments using PBMCs from at least four donors. The percentages of dead cells were assessed as described in **B***.

F. CFSE-stained BV173 target cells were incubated for 4 h with CD16+ NK92 cells in effector:target ratio of 2.5:1, 10 µg/mL OBI and ¼ Cmax concentrations of TKIs. The presented data are the means +/- SEM of at least three independent experiments. The percentages of dead cells were assessed as described in **B.**

G. NK cells were isolated from healthy donors and incubated with ¼ Cmax TKIs and CFSE-stained K562 target cells in effector:target ratio of 10:1 for 4 h without the addition of antibodies. The percentage of dead cells was assessed by flow cytometry as the percentage of CFSE and PI double-positive cells.

The differences between groups in **A-G** were assessed by one-Way ANOVA with Dunnett's post hoc test, *P < 0.05, **P < 0.01, ***P < 0.001.

A
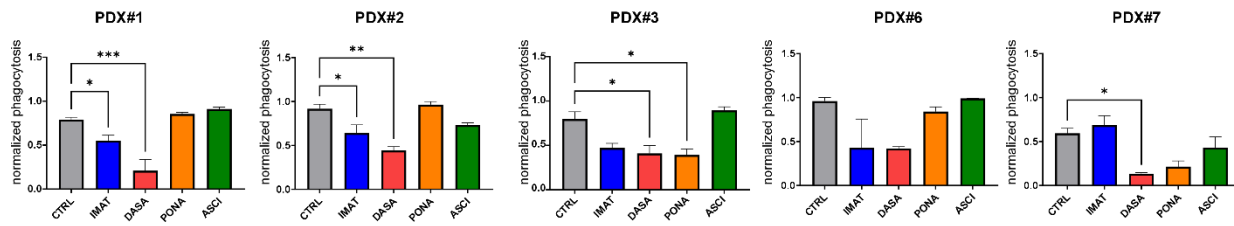
B
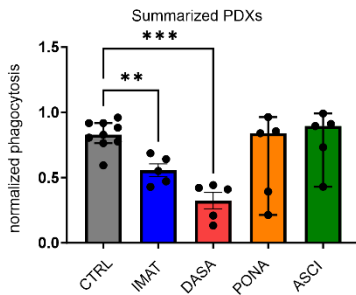
Supplementary figure 7. **Effects of TKIs on RTX-mediated ADCP**.

A. Primary CD20$^+$ BCP-ALL PDXs cells were stained with CFSE and opsonized with 5 µg/ml RTX. Next, the PDXs cells and primary human M1 macrophages were preincubated for 2 h with ¼ Cmax concentrations of TKIs and then co-incubated for 1 h in the presence of ¼ Cmax concentrations of TKIs. The percentage of phagocytosis was assessed by flow cytometry as the fraction of double-positive macrophages. The background phagocytosis was assessed using cetuximab. After background subtraction, phagocytosis was normalized to the highest technical replicate per donor. Differences were calculated using one-way ANOVA followed by Dunnett's multiple comparisons test, $*P < 0.05$, $**P < 0.01$, $***P < 0.001$.

B. Summarized results showing mean ADCP of five PDXs presented in **A** (n=5 PDXs). *P* values were calculated using Welch's ANOVA test followed by Dunnett's T3 test for multiple comparisons, $**P < 0.01$, $***P < 0.001$.

Supplementary methods

Cell culture

Human Ph$^+$ BCP-ALL cell lines (SD1, BV173, TOM1, SUP-B15) were purchased from DSMZ. SD1, BV173, and SUP-B15 were maintained in RPMI 1640 medium (Gibco) supplemented with 10% FBS (HyClone) and 1% penicillin/streptomycin (Sigma-Aldrich). TOM1 cell line was maintained in RPMI 1640 supplemented with 20% FBS (Gibco). NK92 cell line expressing CD16 was cultured in X-Vivo 20 (Lonza) with 5% Human AB serum (Merck). BCP-ALL PDXs were incubated in StemSpan™ SFEM II medium (STEMCELL Technologies), 20% FBS (Gibco) supplemented with 20 ng/mL of recombinant IL-3 (R&D Systems), and 10 ng/mL of recombinant IL-7 (R&D Systems). Peripheral blood mononuclear cells (PBMC) were obtained by Lymphoprep™ (STEMCELL Technologies Germany GmbH) separation from buffy coats obtained from the Regional Blood Center in Warsaw. All cell lines were cultured at 37°C and 5% CO$_2$ and routinely tested for the presence of Mycoplasma DNA to prevent contamination.

Reagents

Chemotherapeutic drugs used for *in vitro* experiments are listed in Supplementary Table 9. L-asparaginase, methylprednisolone and imatinib mesylate were dissolved in water. All other compounds were dissolved in DMSO (Sigma Aldrich). In all experiments, control groups were treated with DMSO. Monoclonal antibodies: RTX (Riximyo, Sandoz GmbH), cetuximab (Erbitux, Eli Lilly and Company) and obinutuzumab (Gazyvaro, Roche) were a kind gift from Institute of Hematology and Transfusion Medicine.

Analysis of the *MS4A1* mRNA levels

Primary cells
Total RNA was isolated from lymphoblasts collected at diagnosis and resuspended in TRIzol solution using chloroform extraction according to the Invitrogen protocol followed by Qiamp RNAeasy mini kit (Qiagen). The concentration and purity of the nucleic acid were determined using NanoDrop Spectrophotometer-8000 (ThermoFisher Scientific). The complementary DNA (cDNA) was obtained with the use of the High-Capacity cDNA Reverse Transcription Kit (ThermoFisher). The expression level of the CD20-encoding gene *MS4A1* was assessed by q-PCR using AriaMx Real-time PCR System (Agilent). Real-time PCR for *MS4A1* (CD20) was performed according to the manufacturer's instruction using 60 ng of the cDNA, TaqMan Gene Expression Master Mix (ThermoFisher Scientific), and the TaqMan gene expression assay (Hs01096429_m1;ThermoFisher Scientific). *B2M* was used as a housekeeping gene (Hs00187842_m1;ThermoFisher Scientific). Results were analyzed with the use of the AriaMX software.

Cell lines
Total RNA was isolated from cell lines after 24 h incubation with TKIs, according to the Invitrogen protocol followed by Qiamp RNAeasy mini kit (Qiagen). The concentration and purity of the nucleic acid were determined using NanoDrop Spectrophotometer-8000 (ThermoFisher Scientific). The complementary DNA (cDNA) was obtained with the use of the Maxima First Strand cDNA Synthesis Kit for RT-qPCR (ThermoFisher Scientific). The levels of the *MSRA1* gene were assessed by q-PCR using LightCycler® 480 SYBR Green I Master (Roche). The reaction was performed using 12.5 ng of the cDNA. *RLP29* and *GUSB* were used as housekeeping genes. The relative expression levels of genes were calculated using LightCycler 480 Software 1.5 (Roche) as described in [2]. Primer sequences are listed in Supplementary Table 11.

Assessment of CD20 levels by flow cytometry in primary samples

Adult patients

Bone marrow or peripheral blood samples from all patients were analyzed at diagnosis and underwent a follow-up assessment (MRD) after 50-85 days. The material processing was carried out in accordance with Euro Flow guidelines. Briefly: bone marrow/peripheral blood samples were incubated with a mixture of fluorescence-labeled mAbs for 15 min at room temperature in the dark. The samples were stained with the following combination of mAbs: CD45 V500 (clone HI30), CD20 V450 (clone 2H7), CD81 FITC (clone JS-81), CD22 PE (clone S-HCL-1), CD34 Per-Cy5.5 (clone 8G12), CD19 PE-Cy7 (clone J3-119), CD10 APC (clone HI10A), CD38 APC (clone HB7) (BD Biosciences). Lysis of red blood cells was done using BD Pharm Lyse solution (BD Biosciences). Immunophenotyping at diagnosis was performed by collecting 100,000 cellular events. Leukemic cells were identified using a gate that included all CD19$^+$ cells on a CD19/SSC-A dot plot. The threshold was set according to the upper limit of the background fluorescence of lymphoid cells not expressing B-cell markers. All flow cytometric analyses were carried out on a FACS Canto II flow cytometer (BD Biosciences) at the Institute of Hematology and Transfusion Medicine in Warsaw. The instrument was aligned and calibrated daily with the use of CaliBRITE beads (BD FACSDiva CS&T IVD Beads, BD Biosciences) according to the manufacturer's instructions.

Pediatric patients

Bone marrow samples from all patients were analyzed at the time of diagnosis and underwent a follow-up assessment after 15 days of treatment (referred to as MRD15). The samples were stained with the following combination of mAbs: CD45 V500 (clone HI30), CD19 PE-Cy7 (clone J3-119), CD34 Per-Cy5.5 (clone 8G12) (BD Biosciences), and CD20-Pacific Blue (clone 2H7), (Biolegend). Bone marrow samples were incubated with a mixture of fluorescently-labeled mAbs for 15 min at room temperature in the dark. Lysis of mature red blood cells was done using BD Pharm Lyse solution (BD Bioscience). Then, the samples were washed with Cell Wash solution (BD Biosciences). Leukemic cells were identified using a gate that included all CD19$^+$ cells, with low SSC and low to dim CD45 expression. All flow cytometric analyses were carried out on a FACS Canto or FACS Lyric flow cytometer (BD Biosciences, San Jose, CA, USA) at the Department of Pediatric Hematology and Oncology, Medical University of Silesia in Zabrze.

PDXs generation

For generation of patient-derived xenografts (PDXs), primary BCP-ALL cells isolated from the bone marrow of pediatric and adult BCP-ALL patients were implanted *i.v.* to NOD.Cg-Prkdcscid Il2rgtm1Wjl/SzJ (NSG) mice (The Jackson Laboratory), as previously described in [3]. All *in vivo* procedures were approved by the Local Ethics Committee of the University of Life Sciences, Warsaw, Poland and Warsaw University, Warsaw (WAW2/095/2019, 639/2018). Details of the specific PDXs are listed in Supplementary Table 7. The measurements of CD20 percentages in various PDXs and their generations are presented in Supplementary Figure 4C.

Assessment of CD20 levels after drug treatment

BCP-ALL cell lines and PDXs were incubated for 48 h in their medium with the following drugs: (IMAT - imatinib; DASA - dasatinib; PONA - ponatinib; ASCI - asciminib; ARAC - cytarabine; DEX - dexamethasone; M-PRED - methylprednisolone; DNR - daunorubicin; LASP - L-asparaginase; MTX - methotrexate; VCR - vincristine; 4-CYCL - 4-hydroperoxycyclophosphamide). The concentrations of drugs used for the immunophenotyping experiments were selected through cytotoxicity screening in order to establish EC50 doses corresponding to each cell line. The concentrations tested were not higher than Cmax concentrations according to pharmacokinetics

literature search. If a highest achievable concentration of certain drug did not reach the cytotoxic effect of EC50, Cmax concentration were used (see Suppl. Table 9). Next, the cells were rinsed in PBS/0.1% BSA, incubated for 15 minutes with human F_C block (BD Biosciences), and stained with anti-CD20 antibody at a dilution 1:20 (see Suppl. Table 10). 7-AAD (Thermo Fisher) was added before the flow cytometry analysis to exclude dead cells. The results on the heatmap are the log of the mean fluorescence (geometric mean) values normalized to control (fold over control) after the deduction of isotype control background.

Natural cytotoxicity

NK cell were isolated using EasySep™ Human NK Cell Isolation Kit Next (StemCell Technologies). K562 target cells were labeled with CellTrace™ CFSE Cell Proliferation Kit (Thermo Fisher) at a final concentration of 0.25 µM for 10 min at 37°C before the assay. Effector and target cells in the effector:target ratio of 10:1 were coincubated at 37°C for 4 h in presence of TKIs at their maximal clinically achievable concentration (Cmax) and ¼ of Cmax.

CDC assay

BCP-ALL cell lines or PDX were preincubated for 48 h with TKIs prior to the CDC assay. After 48 h, the live cells were separated from the dead using Lymphoprep™ (STEMCELL) and subjected to 10% (PDX#2) or 20% (BV173) human AB serum collected from a healthy donor and 20 µg/mL RTX for 1 h. After the incubation, the cells were stained using Propidium Iodide (PI) viability reagent and analyzed using flow cytometry. Percentages of dead cells in the samples without RTX were used as a background control.

ADCC assay

Model with target cell preincubation

BV173 cells (target cells) were stained with CFSE at a final concentration of 3.5 µM for 10 min at 37°C. Target cells were then preincubated for 48 h at 37°C with Cmax or ¼ of Cmax concentrations of TKIs. After the incubation period, live cells were separated from dead cells using Lymphoprep™ (STEMCELL) density gradient medium. Next, the cells were coincubated on a 96-well plate with NK92 cells in the effector:target ratio of 2.5:1 with or without RTX (10 µg/mL) and TKIs (Cmax, ¼ Cmax) for 4 hours. The percentage of cytotoxicity was calculated in the CFSE-positive population, using 7-AAD.

Model without target cell preincubation

BV173 targets: BV173 cells (target cells) were stained with CFSE at a final concentration of 3.5 µM for 10 min at 37°C. Next, the cells were coincubated on a 96-well plate with NK92 cells in the effector:target ratio of 2.5:1 with or without RTX (10 µg/mL) or OBI (10 µg/mL) and TKIs (Cmax, ¼ Cmax). The percentage of cytotoxicity was calculated in the CFSE-positive population using 7-AAD.

SD1 targets: Human PBMC were obtained from buffy coats as described above. SD1 cells (target cells) were labeled with CFSE (ThermoFisher) at a final concentration of 1 µM for 10 min at 37°C before the cytotoxicity assay. Target and effector cells were coincubated at 37°C for 4 h in the presence of TKIs at their maximal clinically achievable concentration (Cmax) and ¼ of Cmax, in the effector:target ratio of 25:1.

Differentiation of macrophages from peripheral blood monocytes and M1 polarization

For the generation of monocyte-derived macrophages (MDMs) from PBMC, the cells were cultured in RPMI 1640 supplemented with 10% FBS, 1% penicilin/streptomycin and 1% sodium pyruvate. PBMC from healthy donors were isolated as described above. For monocyte isolation, 5×10^6 PBMCs were seeded in 100/20 mm Advanced Tissue Culture Dish (Greiner Bio-One) and allowed to adhere at 5% CO_2, 37°C for 2 h in their medium supplemented with 1% human AB serum (Sigma-Aldrich). Non-adherent cells were removed by washing the plate with medium and discarding it. Adherent cells were stored overnight at 5% CO_2, 37°C in fresh medium and subsequently supplemented with 100 ng/mL human Macrophage Colony Stimulating Factor (M-CSF)(BD Biosciences). After 48 h, the plate was washed thoroughly with medium, which was then removed and replaced with fresh medium supplemented with 100 ng/mL M-CSF. After next 48 h, the medium was removed, the cells were washed thoroughly with PBS, and covered with 5 mL of non-enzymatic cell dissociation solution Cellstripper™ (Corning) for 15 min at 37°. After dissociation and gentle scraping of the plate bottom using a sterile plunger of 1 mL BD Plastipak Syringe (BD Biosciences), cells were rinsed with PBS, counted, and seeded onto a 96-well, flat-bottom tissue culture-treated plate in their medium, supplemented with 100 ng/mL M-CSF, 10 ng/mL of IFN-γ and 2 ng/mL of LPS in the density of 100,000 cells in 100 µL per well. After 24 h of incubation at 5% CO_2, 37°C, the medium was gently removed from wells using a multi-channel pipette and replaced with fresh medium supplemented with the same concentration of differentiating factors. The cells were incubated at 5% CO_2, 37°C for an additional 24 h prior to the antibody-dependent phagocytosis (ADCP) assay.

Immunoblots

Cell extracts from BCP-ALL cell lines were lysed with RIPA buffer (CD20, α-tubulin) and immunoblotted as previously described[3]. Antibodies used are listed in Supplementary Table 10.

In vitro degranulation assay

NK cell were isolated using EasySep™ Human NK Cell Isolation Kit Next (StemCell Technologies). 100,000 NK cells and 100,000 K562 target cells were placed onto wells of 96-well plate. The cells were subsequently treated with GolgiStop™ Protein Transport Inhibitor (BD Biosciences) to inhibit the surface CD107a recycling and an anti-CD107a APC antibody was added to each well. The cells were then incubated for 4 hours in 37°C in presence of Cmax concentrations of TKIs. Samples were stained using BD Fixable Viability Stain 510 (BD Biosciences) and antibodies against CD56. The percentage of degranulation was determined within live CD56$^+$ cells, with background values subtracted. These background values were obtained from samples containing NK cells but lacking target cells.

Statistical analysis and data visualization

Statistical analyses and data visualization were performed using Prism 9.5.1 software (GraphPad Software). The type of statistical test and appropriate post-hoc corrections are described in Figure legends. *P* values were considered statistically significant when lower than 0.05 (*$P < 0.05$, **$P < 0.01$, ***$P < 0.001$). The Experimental schemes of the CDC, ADCC and natural cytotoxicity assays (Figure 3), as well as ADCP assay (Figure 5A) and the whole blood *ex vivo* assay for testing the degranulation of NK cells (Figure 4B) were designed using biorender.com.

Text editing

Authors utilized GPT-3, OpenAI's large-scale language-generation model to enhance the grammatical and lexical quality of this text.

Supplementary Table 1. Drug exposure during the induction phase of the ALL-IC BFM 2009 and AEIOP BFM 2017 protocols.

ALL-IC BFM 2009 Protocol			
Drug	**Route of administration**	**Per-Day Dose**	**Days of Administration**
Induction Phase of Protocol I			
Prednisone	*p.o.*	60 mg/m^2	1-28
Vincristine	*i.v.*	1.5 mg/m^2 (max. 2 mg)	8, 15, 22, 29
Daunorubicin	*p.i.* over 1 hour	30 mg/m^2	8, 15 (22 and 29 in IR and HR patients)
L-asparaginase (L-ASP)	*p.i.* over 1 hour	5,000 IU/m^2	12, 15, 18, 21, 24, 27, 30, 33
Methotrexate	*i.t.*	Age-adjusted dose: < 1 year: 6 mg <1 -2) years: 8 mg <2 -3) years: 10 mg ≥ 3 years: 12 mg	1, 12, 33*
AIEOP- BFM 2017 Protocol			
Protocol IA-Pred.(pB-ALL patients or unknown immunophenotype), Induction Phase			
Prednisone (alternatively Prednisolone)	*p.o./i.v.*	60 mg/m^2	1-28
Vincristine	*i.v.*	1.5 mg/m^2 (max. 2 mg)	8, 15, 22, 29
Daunorubicin	*p.i.* over 1 hour	30 mg/m^2	8,15,22,29
PEG-L-ASP **	*p.i.* over 2 hours	2 500 IU/m^2 (max. 3 750 IU)	12,26
Methotrexate	*i.t.*	Age-adjusted dose: < 1 year: 6 mg <1 -2) years: 8 mg <2 -3) years: 10 mg ≥ 3 years: 12 mg	12,33***

p.i. (per infusionem) - administered through controlled continuous infusion, *p.o.* (*per os*) – administered orally, *i.v.* - administered intravenously, *i.t.* - administered by intrathecal injection

* If CNS positive, or CNS neg. but blasts in CSF, or traumatic LP: additional MTX IT on day 18/27
** In case of hypersensitivity to PEG-L-Asparaginase, Erwinia Asparaginase is given at a dosage of 20 000 IU/m2/dose p.i. (1 h) or i.m. every second day for the remaining days of scheduled Asparaginase treatment, i.e. until two weeks after the last scheduled PEG-L-Asparaginase dose in this element.
*** In case of initial CNS3 status additional intrathecal Methotrexate is given on days 19 and 26

Supplementary Table 2. Drug exposure during the induction phase of the EsPhALL2017/COGAALL1631 protocol

EsPhALL2017/COGAALL1631 Protocol			
Drug	Route of administration	Per-Day Dose	Days of Administration
Induction IA Part 2*			
Prednisone/Prednisolone	*p.o.*	60 mg/m^2	15-28
Vincristine	*i.v.* over 1 min	1.5 mg/m^2 (max. 2 mg)	15, 22
Daunorubicin	*i.v.* over 1-15 mins	25 mg/m^2	15, 22
Methotrexate	*i.t.*	Age-adjusted dose: <1 -2) years: 8 mg <2 -3) years: 10 mg ≥ 3 years: 12 mg	29
Imatinib	*p.o.*	340 mg/m^2 (max. 800 mg)	Daily
Induction IB			
Cyclophosphamide	*i.v.* over 30-60 mins	1000 mg/m^2	1, 28
Mercaptopurine	*p.o.*	60 mg/m^2	1-28
Cytarabine	*i.v.* over 1-39 mins or *s.c.*	75 mg/m^2	3-6, 10-13, 17-20, 24-27
Methotrexate	*i.t.*	Age-adjusted dose: <1 -2) years: 8 mg <2 -3) years: 10 mg ≥ 3 years: 12 mg	10, 24
Imatinib**	*p.o.*	340 mg/m^2 (max. 800 mg)	Daily

p.o. (*per os*) – administered orally, *i.v.* - administered intravenously, *i.t.* - administered by intrathecal injection, *s.c.* - administered subcutaneously

*Prior to BCR::ABL1 detection and qualification to EsPhALL2017/COGALL1631 protocol (10-15 days from initial diagnosis), patients were treated with induction treatment of the default front-line ALL treatment (ALL-IC BFM 2009 or AIEOP- BFM 2017).

** Patients begun imatinib once daily at the time of trial enrollment, which was no later than Day 15.

Supplementary Table 3. Drug exposure during the pretreatment and induction phases of PALG ALL6 protocol

Drug	Route of administration	Per-Day Dose	Days of administration
PALG ALL6 protocol			
Ph⁻ patients			
<55 y/o			
Pretreatment			
Prednisone	p.o.	60 mg/m² (≥40 y/o – 40mg/m²)	-7 to -1
Liposomal cytarabine	i.t.	50 mg	1x between -7 and -3
Induction			
Prednisone	p.o./i.v.	60 mg/m² (≥40 y/o – 40mg/m²)	1-28
Vincristine	i.v.	2 mg	1, 8, 15, 22
Daunorubicin	i.v.	50 mg/ m² (≥40 y/o – 40 mg/m2)	1, 8, 15, 22
Peg-asparaginase	i.v.	1,000 IU/m²	13
Liposomal cytarabine	i.t.	50 mg	10
≥55 y/o			
Pretreatment			
Dexamethasone	p.o.	10 mg/m²	-5 to -1
Methotrexate	i.t.	12 mg	1x between -5 and -1
Induction			
Dexamethasone	p.o.	10 mg/m²	1 to 7, 15 to 21
Vincristine	i.v.	2 mg	1, 8, 15, 22
Daunorubicin	i.v.	30 mg/m²	1, 8, 15, 22
Peg-asparaginase	i.v.	1,000 IU/m²	10
Methotrexate/Cytarabine/Dexamethasone	i.t.	12 mg/40 mg/4mg	12, 20, 27, 34
Ph⁺ patients			
<55 y/o			
Pretreatment			
Prednisone	p.o.	60 mg/m² (≥40 y/o – 40mg/m²)	-7 to -1
Liposomal cytarabine	i.t.	50 mg	1x between -7 and -3
Induction			
Prednisone	p.o.	60 mg/m² (≥40 y/o – 40mg/m²)	1-28
Vincristine	i.v.	2 mg	1, 8, 15, 22
Daunorubicin	i.v.	40 mg/ m²	1, 8, 15
Liposomal cytarabine	i.t.	50 mg	10
Imatinib	p.o.	600 mg	Daily from day 1
Dasatinib*	p.o.	100 – 140 mg	Daily
≥55 y/o			
Pretreatment			
Dexamethasone	i.v.	10 mg/m²	-5 to -1
Methotrexate	i.t.	12 mg	1x between -5 and -1
Induction			
Dexamethasone	p.o.	10 mg/m²	1-2, 8-11, 15-18, 22-25
Vincristine	i.v.	1 mg	1, 8, 15, 22
Methotrexate/Cytarabine/Dexamethasone	i.t.	12 mg/40 mg/4mg	12, 20, 27, 34
Imatinib	p.o.	600 mg	Daily from day 1
Dasatinib*	p.o.	100 mg	Daily

* In case of imatinib resistance or intolerance

Supplementary Table 4: Drug exposure during the pretreatment and induction phases of PALG ALL7 protocol

PALG ALL7 protocol			
Drug	**Route of administration**	**Single dose**	**Days of administration**
Ph⁻ patients			
Pretreatment			
Dexamethasone	*p.o.*	10 mg/m²	-5 to -1
Methotrexate/Dexamethasone	*i.t.*	15 mg/4 mg	1x between -5 and -1
Induction			
Dexamethasone	*p.o./i.v.*	40 mg (≥70 y/o – 20mg)	1-2, 8-9, 15-16, 22-23
Vincristine	*i.v.*	2 mg	1, 8, 15, 22
Daunorubicin	*i.v.*	50 mg/ m² (≥40 y/o – 40 mg/m2; ≥55 y/o – 30 mg/m2)	1, 8, 15, 22
Peg-asparaginase	*i.v.*	2,000 IU/m² (max. 3750 IU) (≥55 y/o – 1,000 IU/m²)	20
Methotrexate/Cytarabine/Dexamethasone	*i.t.*	15 mg/40 mg/4mg	13, 27
Rituximab*	*i.v.*	375 mg/m2	1, 8
Ph⁺ patients			
Pretreatment			
Dexamethasone	*i.v.*	12 mg/ m² (≥55 y/o – 10 mg/ m²)	-5 to -1
Methotrexate/Dexamethasone	*i.t.*	15 mg/4 mg	1x between -5 and -1
Induction			
Dexamethasone	*p.o./i.v.*	40 mg (≥70 y/o – 20mg)	1-2, 8-9, 15-16, 22-23
Vincristine	*i.v.*	2 mg (≥55 y/o – 1 mg)	1, 8, 15, 22
Methotrexate/Cytarabine/Dexamethasone	*i.t.*	15 mg/40 mg/4mg	10, 24
Rituximab*	*i.v.*	375 mg/ m²	1, 8
Imatinib	*p.o.*	600 mg	daily from day 1
Dasatinib**	*p.o.*	140 mg	daily
Ponatinib***	*p.o.*	45 mg	daily

* If CD20 is detected on ≥20% blasts
** In case of imatinib resistance or intolerance
*** In case of dasatinib resistance or detection of T315I mutation

Supplementary Table 5: Clinical characteristics of CD20-high and CD20-low patients

	CD20 high	CD20 low	*P value*
n	26	91	-
% of Total	22.22 %	77.78 %	
Treatment protocol			
ALL-IC 2009 (n)	3	7	-
AIEOP-BFM 2017 (n)	23	84	
Sex, n(%)			
Male	15 (57.69 %)	47 (51.65 %)	0.59 **
Female	11 (42.31 %)	44 (48.35 %)	
Age at ALL diagnosis (years)			
Median	5.23 (3.24-10.52)	5 (2.5-7.0)	0.089*
<10	18	76	
10-14	5	12	
15-18	3	3	
WBC (n/ul)			
Median	13465 (3875-36147.5)	14000 (5550-58000)	**0.038***
Unknown/ Missing	10	14	
BM blasts at diagnosis (%)			
20-39	0	0	0.16*
40-59	1	5	
60-79	1	3	
>=80	15	70	
Unknown/ Missing	9	14	
CNS involvement			
CNS1 (n)	17	68	0.50 **
CNS2 (n)	3	5	
CNS3 (n)	2	6	
Unknown/ Missing (n)	4	12	
Steroidoresistance			
Yes (n)	3	5	0.13 **
No (n)	12	63	
Unknown/ Missing (n)	11	23	
FCM-based MRD at day 15			
Positive (>10%) (n)	7	7	**0.003***
Negative (n)	12	66	
Unknown (n)	8	18	
PCR-based MRD at day 33			
Positive (n)	8	32	0.97**
Low, but positive (<10^-4)	7	25	
Negative (n)	5	21	
Unknown/ Failed (n)	6	9/4	
Risk group			
SR (n)	2	16	0.36**
MR (n)	6	33	
HR (n)	6	16	
Unknown/ Missing (n)	12	26	
Complete Remission Achieved			
Yes	15	66	0.52**
No	1	2	

Unknown/ Missing	10	23	
Death			
n	4	3	**0.02****
% of total	15.38 %	3.30 %	
Relapse			
n	4	10	0.54**
% of total	15.38 %	10.99 %	

*U-Mann Whitney test, **-Chi-Square test

Supplementary Table 6: Clinical characteristics of adult BCP-ALL patients

All adult BCP-ALL patients enrolled (n)	**72**
Sex (n)	
Male	32
Female	40
Age at ALL diagnosis (n)	
≥55	26
<55	46
Median (years)	46,5
BCR-ABL status (n)	
Ph+	26
Ph-	46
CD20-positivity (n)	
CD20+	31
CD20-	41
CNS involvement (n)	
Yes	13
No	39
Unknown/Missing	20
CR after induction (n)	
Yes	38
No	7
Unknown/Missing	27

CNS – Central Nervous System; CR – Complete Remission

Supplementary Table 7: Characteristics of patients used for generation of PDXs. Samples were collected at the time of diagnosis.

Sample ID	BCP-ALL subtype	Risk group	Age group	Sex
PDX#1	Ph+	HR	adult	M
PDX#2	Ph+	HR	pediatric	M
PDX#3	Ph+ CML-LBC	HR	adult	F
PDX#4	Ph+	HR	pediatric	M
PDX#5	Ph+	HR	adult	M
PDX#6	Ph+	HR	pediatric	M
PDX#7	Ph-like	HR	pediatric	M

CML LBC – Chronic Myeloid Leukemia Lymphoblastic Crisis

Supplementary Table 8: Characteristics of patients used for *ex vivo* experiments presented in Fig. 4B.

Sample ID	Diagnosis	Treatment	Sex
Ex vivo patient #1	BCP-ALL	DASA 140 mg QD *p.o.*	F
Ex vivo patient #2	CML	DASA 140 mg QD *p.o.*	M
Ex vivo patient #3	CML	ASCI 40 mg BID *p.o.*	M
Ex vivo patient #4	CML	DASA 100 mg QD *p.o.*	F
Ex vivo patient #5	CML	DASA 100 mg QD *p.o.*	M
Ex vivo patient #6	CML	ASCI 40 mg BID *p.o.*	M
Ex vivo patient #7	CML	IMAT 400 mg QD *p.o.*	M
Ex vivo patient #8	CML	IMAT 400 mg QD *p.o.*	F

BCP-ALL – B-Cell Precursor Acute Lymphoblastic Leukemia; CML – Chronic Myeloid Leukemia; QD (*quaque die*) – once a day; *p.o.* (*per os*) – administered orally; BID (*bis in die*) – twice a day

Supplementary Table 9. Selected drugs and concentrations for testing CD20 level changes in BCP-ALL cell lines and functional assays.

Drug	Abbrev.	Concentration [nM]				Supplier
		BV173	SUP-B15	SD1	TOM1	
cytarabine	ARAC	6.25	15	400	500	Selleckchem
dexamethasone sodium phosphate	DEX	200	150	200	200	Abcam
daunorubicin Hcl	DNR	5	10	10	5	Selleckchem
methotrexate	MTX	5	15	5	10000	Sigma Aldrich
vincristine	VCR	0.5	1	0.4	1	Selleckchem
4-hydroperoxy-cyclophosphamide	4-CYCL	120	120	120	1500	Niomech
imatinib mesylate	IMAT (Cmax)	8000	8000	8000	8000	Santa Cruz Biotechnology
	IMAT (¼ Cmax)	2000	2000	2000	2000	
dasatinib	DASA (Cmax)	160	160	160	160	Sigma Aldrich
	DASA (¼ Cmax)	40	40	40	40	
ponatinib	PONA (Cmax)	140	140	140	140	Selleckchem
	PONA (¼ Cmax)	35	35	35	35	
asciminib	ASCI (Cmax)	1600	1600	1600	1600	Selleckchem
	ASCI (¼ Cmax)	400	400	400	400	
Drug	**Abbrev.**	**Concentration [nM]**				**Supplier**
		BV173	SUP-B15	SD1	TOM1	
L-asparaginase	L-ASP	1	0.1	1	10	Servier IP UK Ltd
Drug	**Abbrev.**	**Concentration [nM]**				**Supplier**
		BV173	SUP-B15	SD1	TOM1	
methylprednisolone	M-PRED	50	50	50	50	Pfizer

Supplementary Table 10. Antibodies used in flow cytometry and immunoblotting

Antibody	Clone	Catalog no.	Company
Flow cytometry antibodies			
anti-hCD20 PE	L27	345793	BD Biosciences
anti-hCD3 BV421	UCHT1	562427	BD Biosciences
anti-hCD3 BV510	SK7	740202	BD Biosciences
anti-hCD107a APC	H4A3	641581	BD Biosciences
Western Blot antibodies			
anti-CD20	polyclonal	ab27093	abcam
	EP459Y	ab78237	abcam
anti-α-Tubulin	DM1A	T6199	Sigma-Aldrich

Supplementary Table 11. List of primers used for RT-PCR

Primers	Sequence
MS4A1_F	GAATGGGCTCTTCCACATTGCC
MS4A1_R	TCTCCGTTGCTGCCAGGAGT
RPL_F	CAGCTCAGGCTCCCAAAC
RPL_R	GCACCAGTCCTTCTGTCCTC
GUSB_F	GAAAATATGTGGTTGGAGAGCTCATT
GUSB_R	CGGAGTGAAGATCCCCTTTTTA

Literature

1. Logan AC. Measurable residual disease in acute lymphoblastic leukemia: How low is low enough? Best Pract Res Clin Haematol. 2022 Dec;35(4):101407.

2. Muchowicz A, Firczuk M, Wachowska M, Kujawa M, Jankowska-Steifer E, Gabrysiak M, et al. SK053 triggers tumor cells apoptosis by oxidative stress-mediated endoplasmic reticulum stress. Biochem Pharmacol. 2015 Feb 15;93(4):418–27.

3. Fidyt K, Pastorczak A, Goral A, Szczygiel K, Fendler W, Muchowicz A, et al. Targeting the thioredoxin system as a novel strategy against B-cell acute lymphoblastic leukemia. Mol Oncol. 2019 May;13(5):1180–95.